Some applications of photoluminescence for probing polymer relaxation processes

Part 2

p1

Teresa Dib Zambon Atvars

Instituto de Química

Universidade Estadual de Campinas

Campinas, São Paulo, Brasil

E-mail: tatvars@iqm.unicamp.br

Summer School - Stereochemical Aspects of Novel Materials, UCSB, august 14-27, 2005

Slide 1

p1 ro

prpg, 7/2/2005

outline

- Polymer systems and morphology
- Polymer motions, phase transitions and polymer relaxation processes
- Photoluminescence spectroscopy and polymer relaxation processes
  - fluorescence
  - phosphorescence
  - quenching processes
  - time resolved spectroscopy
- Luminescence in polymers
  - Non-fluorescent polymers (host-guest systems)
  - Polymers modified with luminescent groups
  - Intrinsically luminescent polymers
  - Conjugated luminescent polymers
  - Electroluminescence and photoluminescence

Types of luminescent polymers : 1. non-fluorescent polymers (host-guest systems)

- **Amorphous materials**
- **Semicrystalline polymers**

How the guest interacts with the polymer?
Which site is the guest sensing?

Guest in semicrystalline polymers

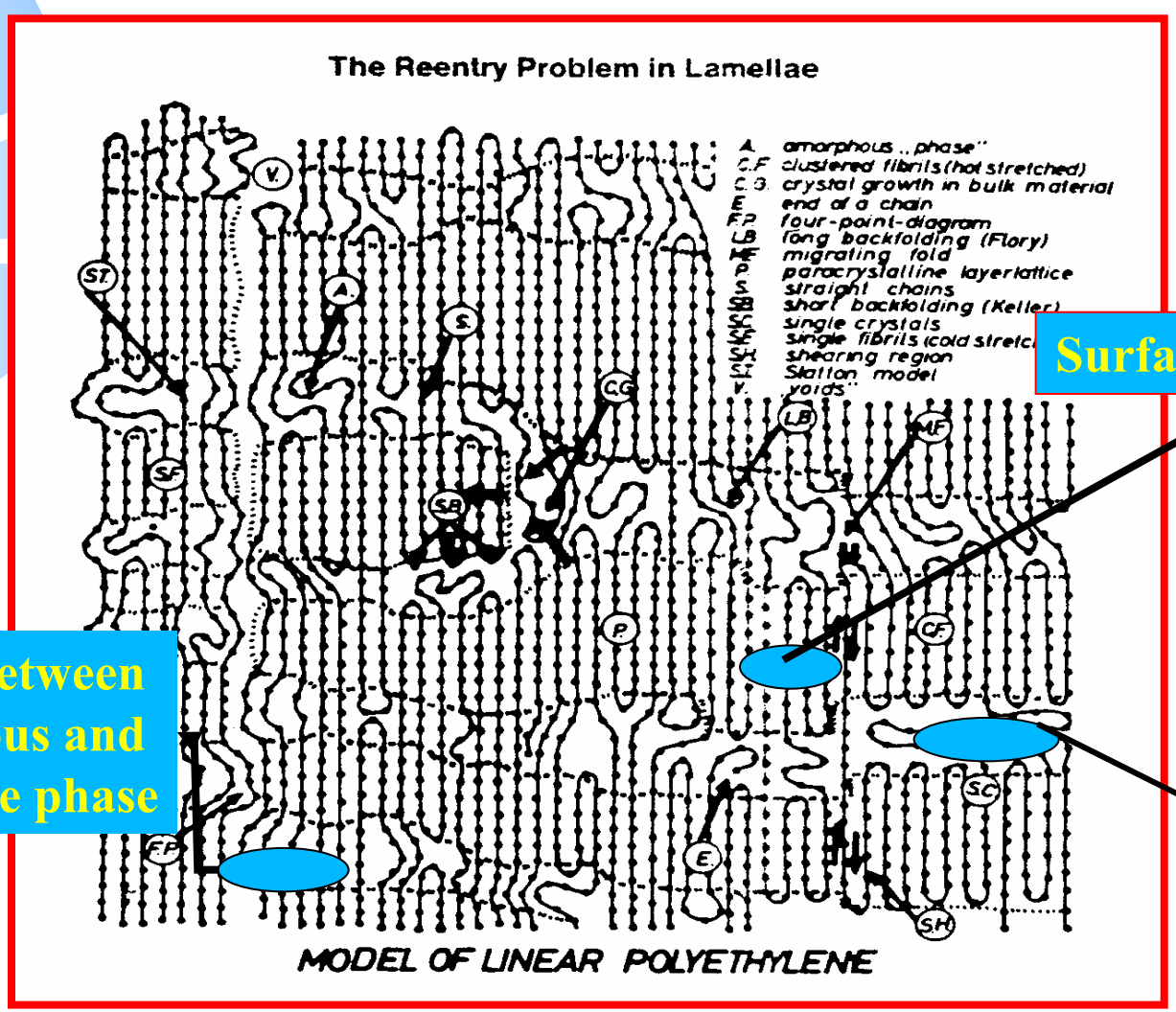

Surface of a lamellae

Interfase between amorfous and crystalline phase

Amorphous region

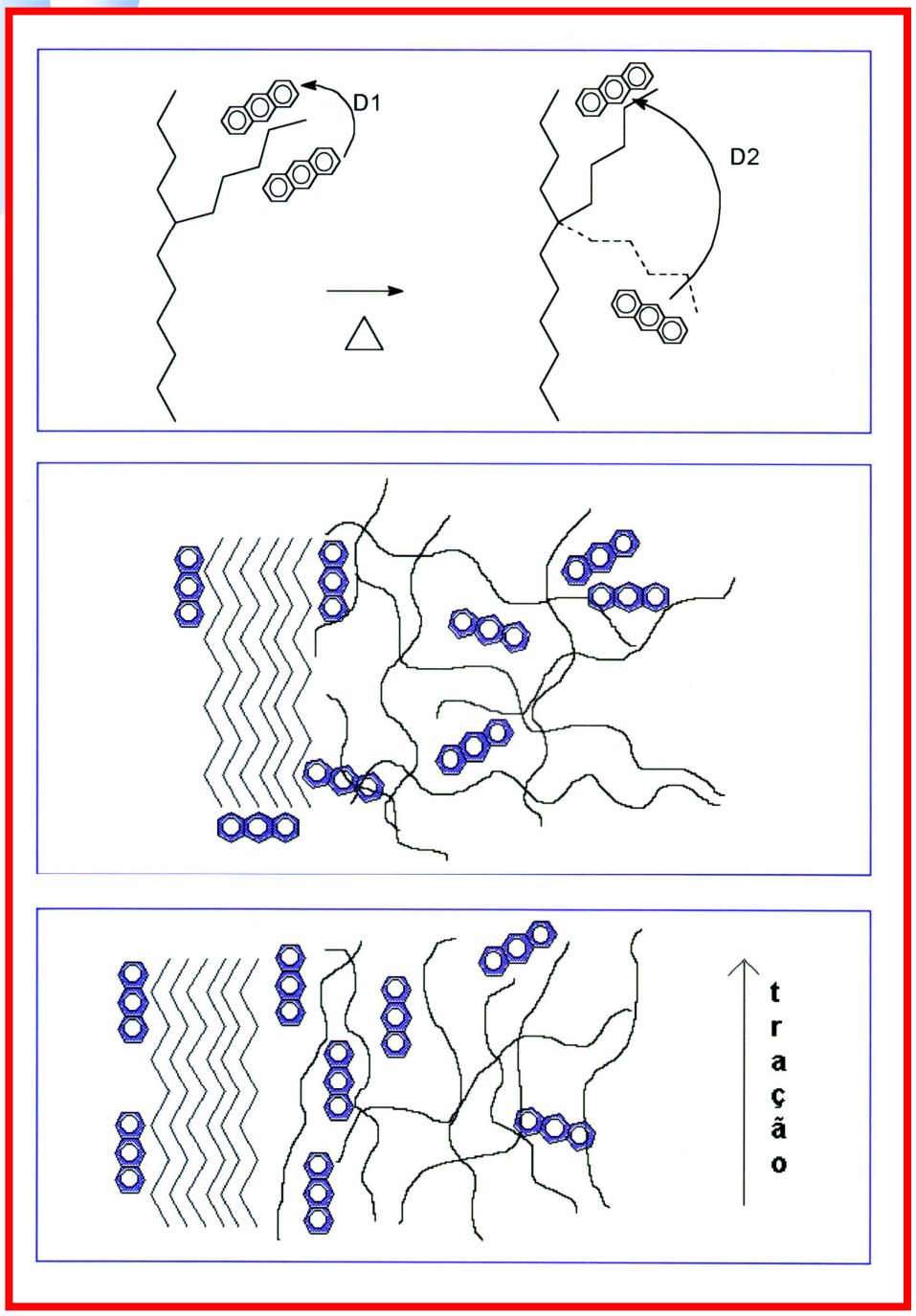

Probing orientation in stretched materials

Molecules changes from one site to other
and can be preferentially oriented in the stretching direction

They can sense the new environment

Relaxation processes in oriented polymers

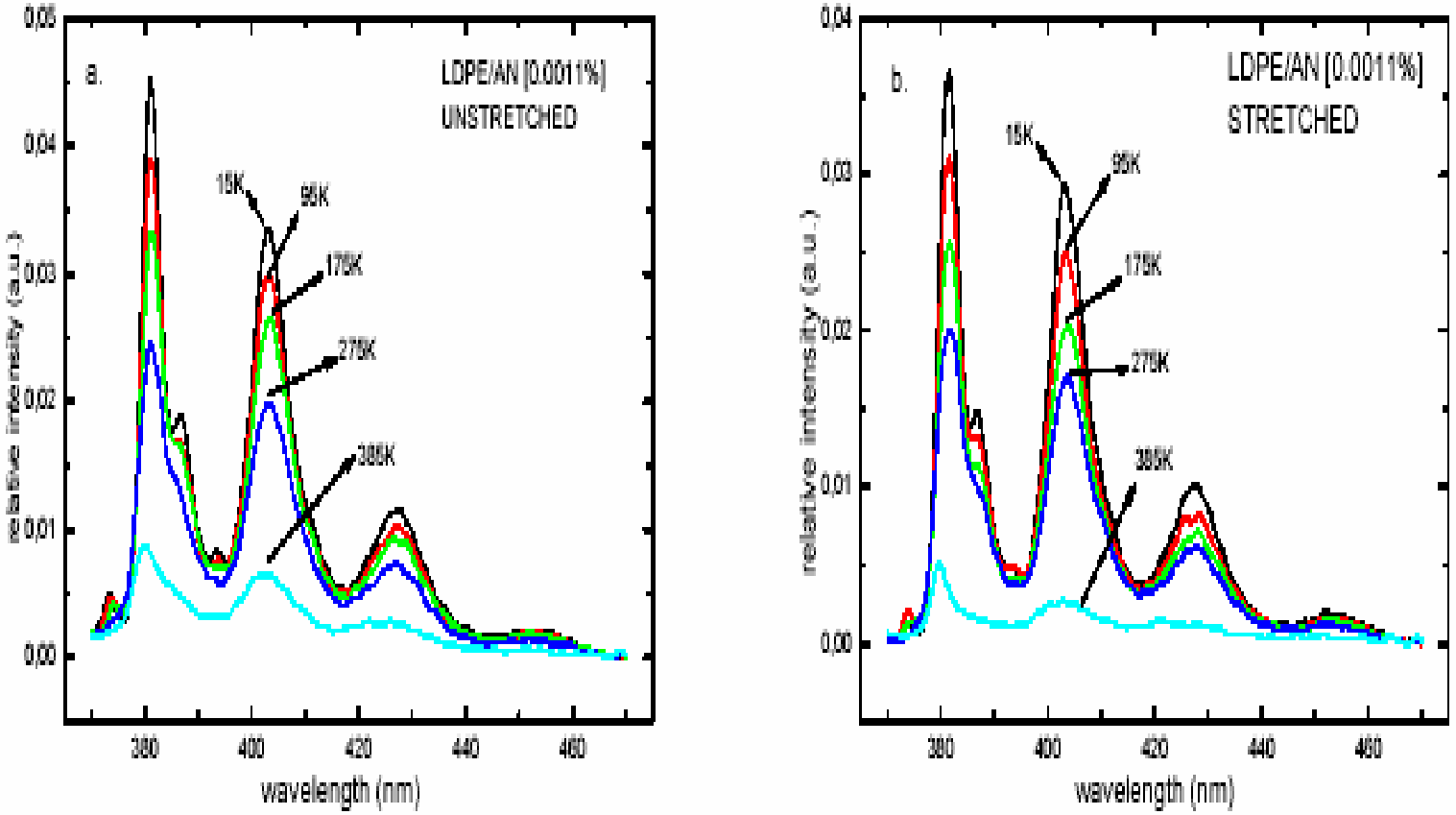

Talhavini et al. Polymer, 1986

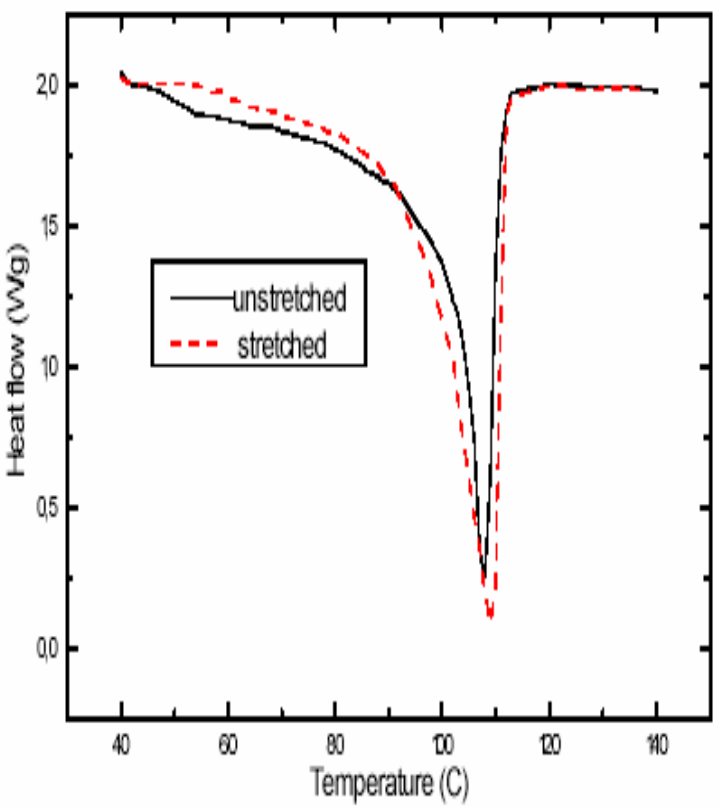
Heat flow (W/g)
Temperature (C)
unstretched
stretched
2,0
1,5
1,0
0,5
0,0
40
60
80
100
120
140

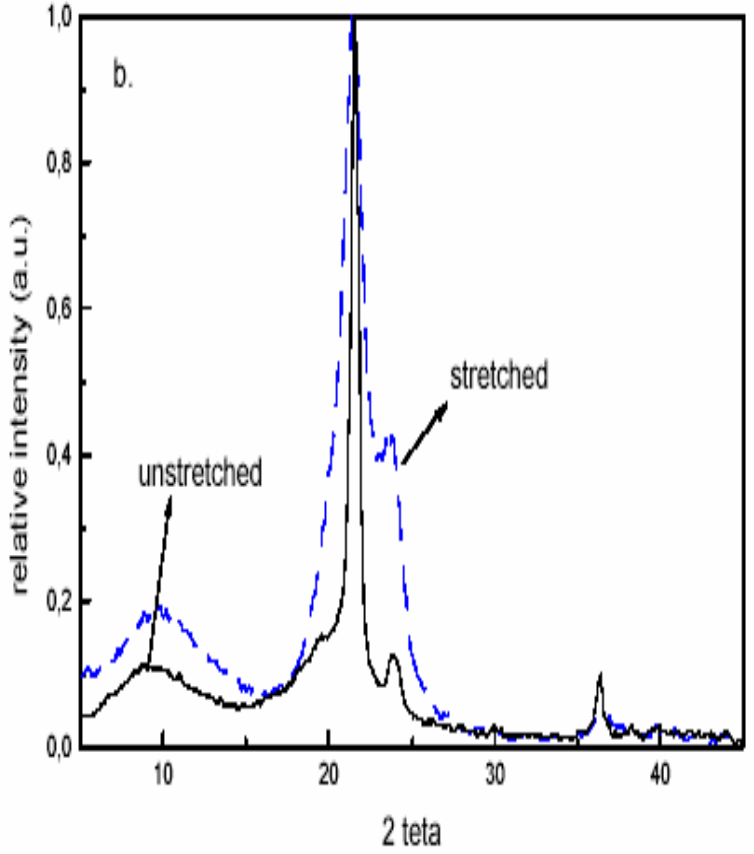
b.
relative intensity (a.u.)
2 teta
unstretched
stretched
1,0
0,8
0,6
0,4
0,2
0,0
10
20
30
40

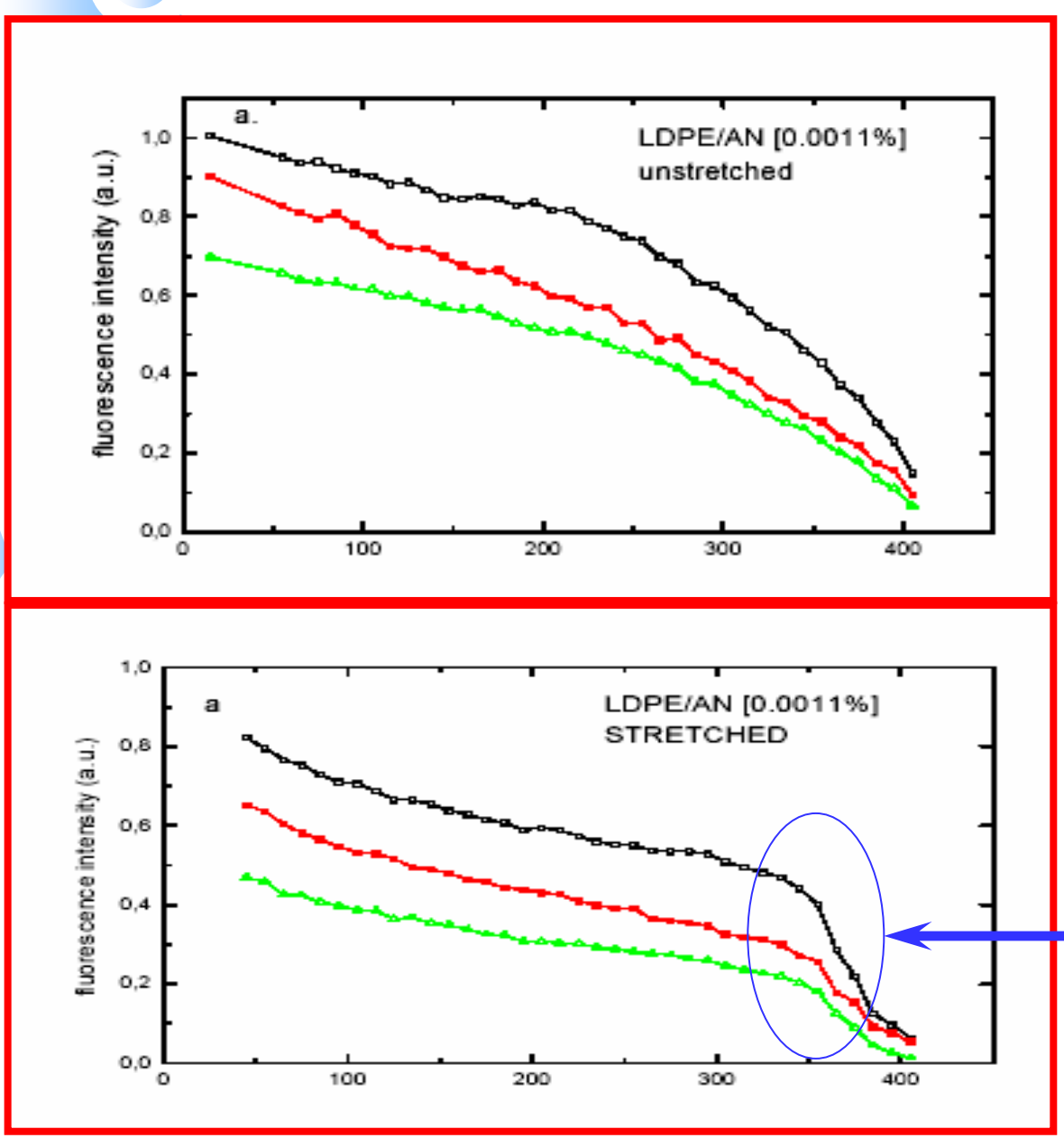

Relaxation processes associated with the interface crystalline amorphous interface are more defined

There is a larger population of anthracene molecules located in the interface compared with non-stretched material

α-relaxation process

Talhavini, et al, Polymer 1986

How important is the distance for a guest sensor?

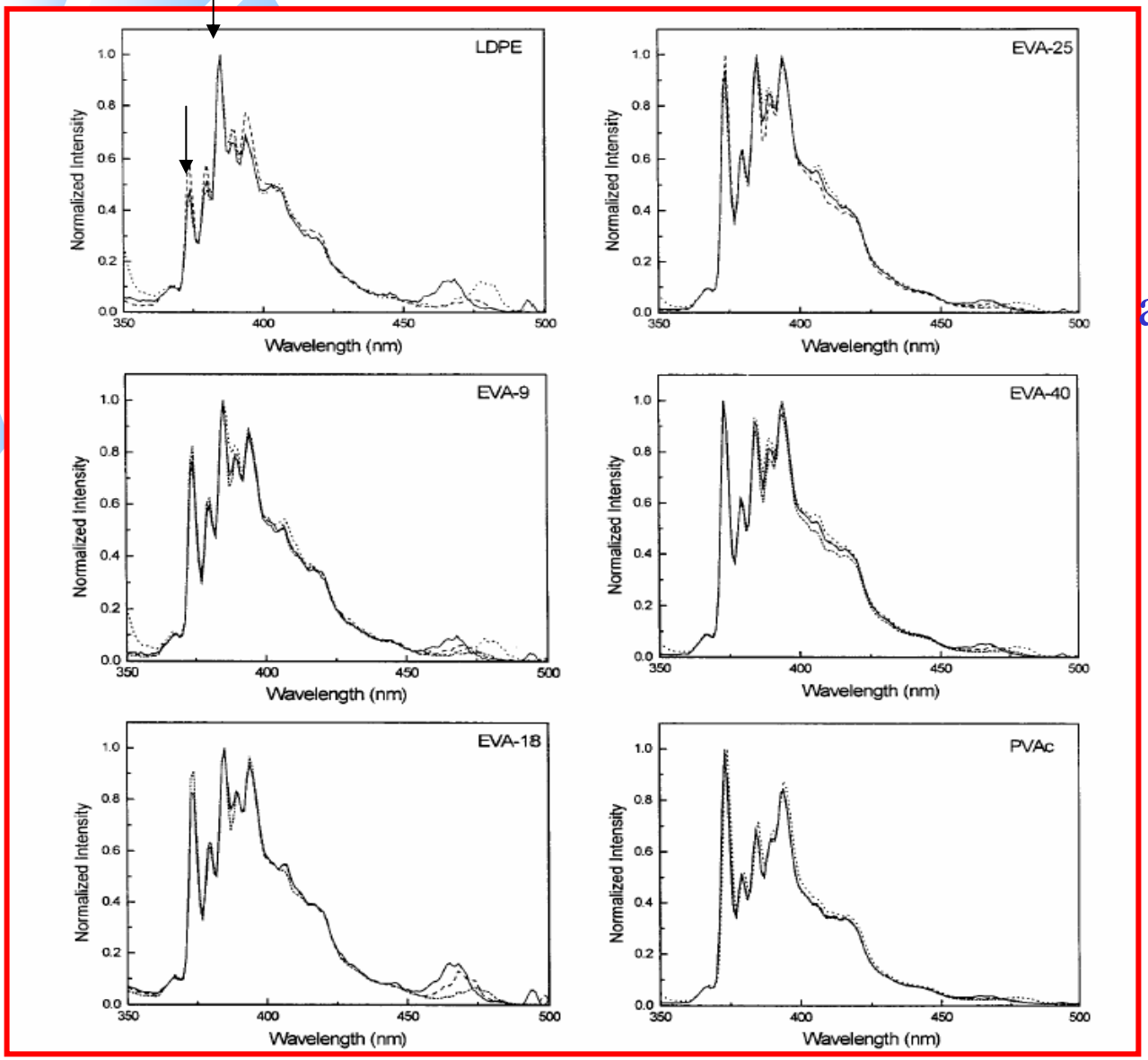

Pyrene in LDPE and some coplolymers with vinyl acetate (EVA)

I_I/I_{III} ratio changes

Lifetimes also change

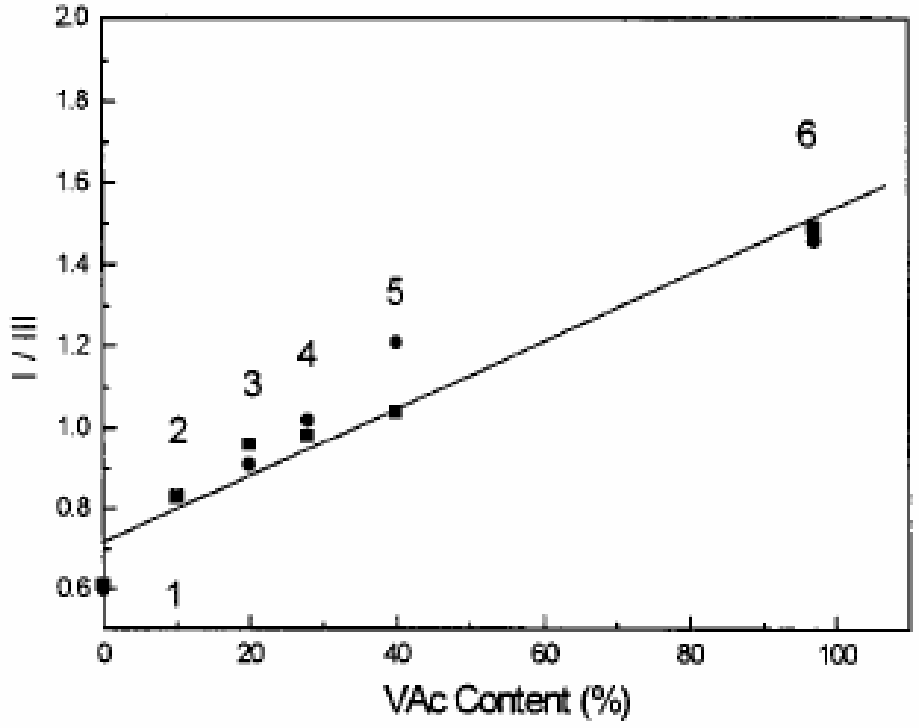

Linear correlation with lifetime and I_I/I_{III} ratio because the random distribution of the polar groups

TABLE 2: Decay Constants τ_F (ns) and Vibrational Intensity Ratios I/III for Fluorescence of Pyrene Sorbed on the Surface (S) and in the Bulk (B) of Polymer Films. λ_{Em} = 393 Nm, λ_{Ex} = 336 nm

	LDPE		EVA-9		EVA-18		EVA-25		EVA-40		PVAc	
	S	B	S	B	S	B	S	B	S	B	S	B
I/III	0.61	0.60	0.83	0.83	0.96	0.91	0.98	1.02	1.04	1.21	1.49	1.46
τ_F (ns)	395 ± 1	392 ± 3	373 ± 3	370 ± 2	359 ± 1	358±2	346±2	347±2	352±1	348 ± 1	311 ± 3	299±1

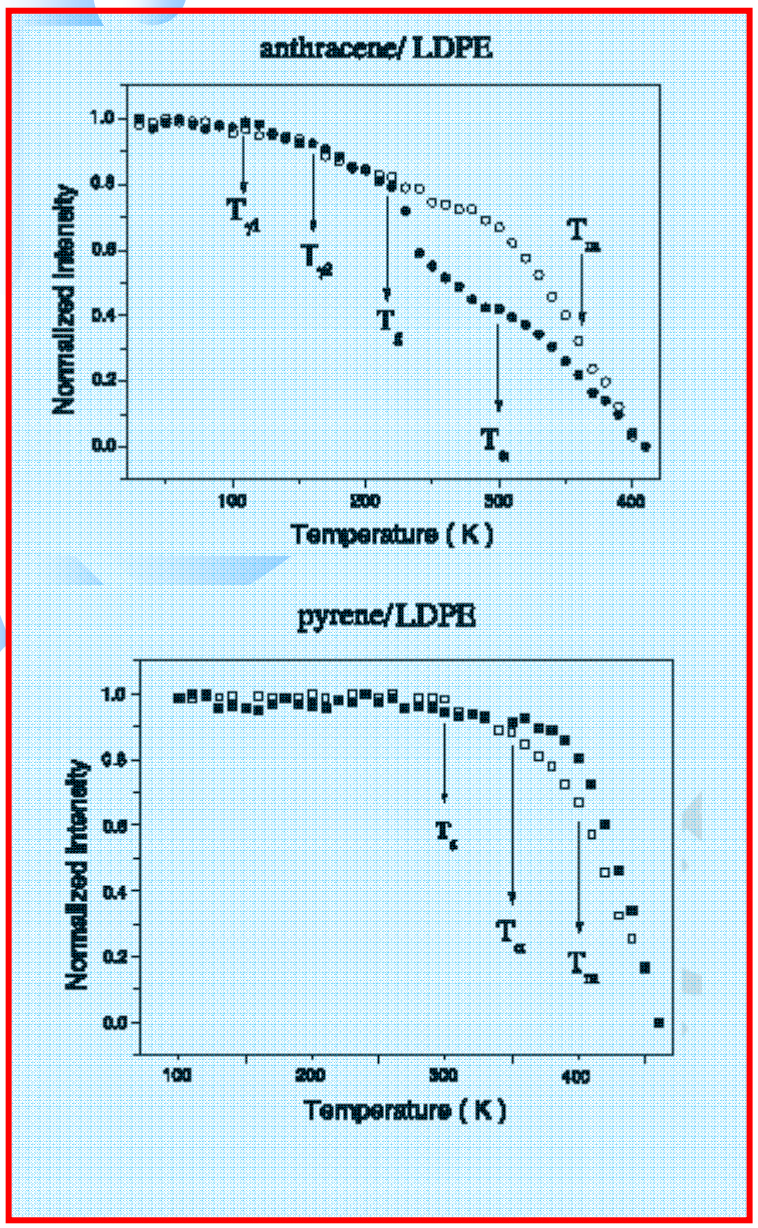

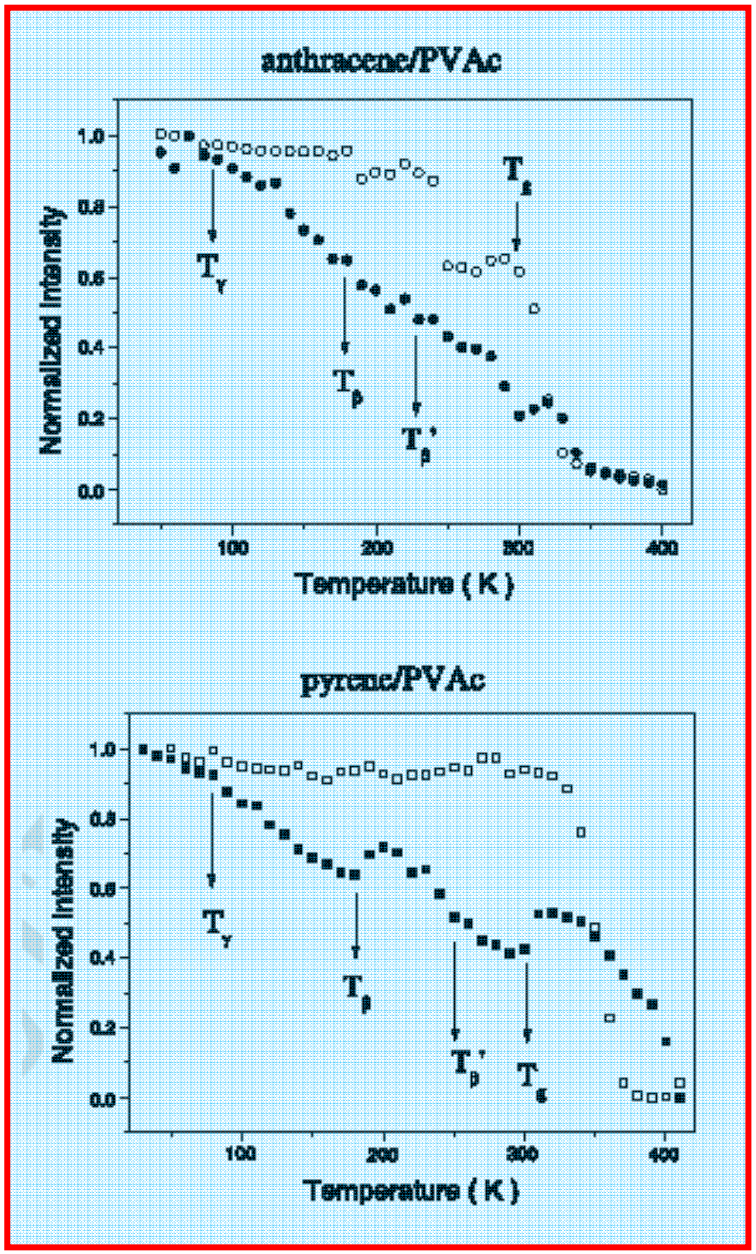

1st (open) and 2nd run (dark)

Yamaki, Eur. Polym. J., 2002

Transition and relaxation temperatures (K) (from the data shown in Figs. 4 and 5), for pyrene and anthracene sorbed in LDPE and PVAc

polymer	T (K)	Assignments
LDPE	$T_{\gamma 1} = 110$	Motions of methylenic segments in the amorphous phase [18,19,21,32]
	$T_{\gamma 2} = 160$	Motions of folded chains in the interfacial regions [32]
	$T_g = 220–250$	Glass transition [18–21,32–39]
	$T_\alpha = 300$	Motions of the segments on the surface of the crystals [18–21,32–39]
	$T_m = 360$	Melting point
PVAc	$T_\gamma = 80–90$	Motions of end groups
	$T_\beta = 180–190$	Small amplitude rotary motions of one or two monomeric units in an amorphous region [40–46]
	$T_{\beta'} = 240–250$	Rotation of the ester group leading to a *cis–trans* isomerization [9]
	$T_g = 300–310$	Glass transition [40]

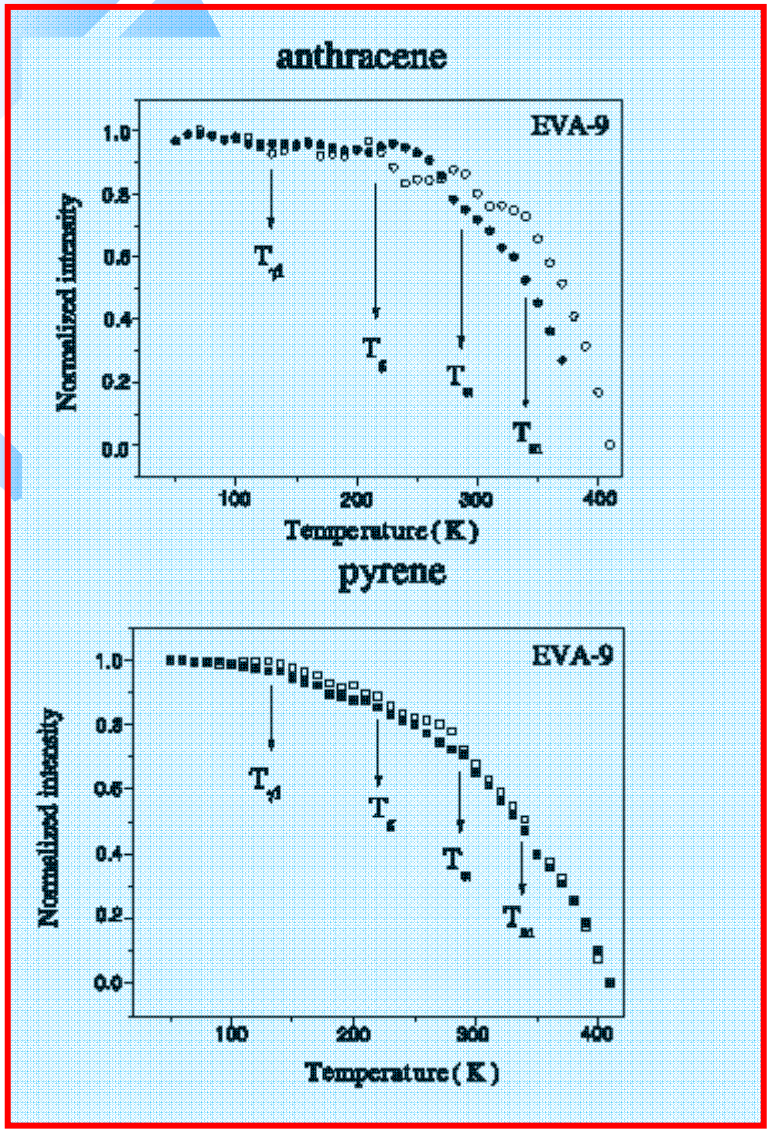

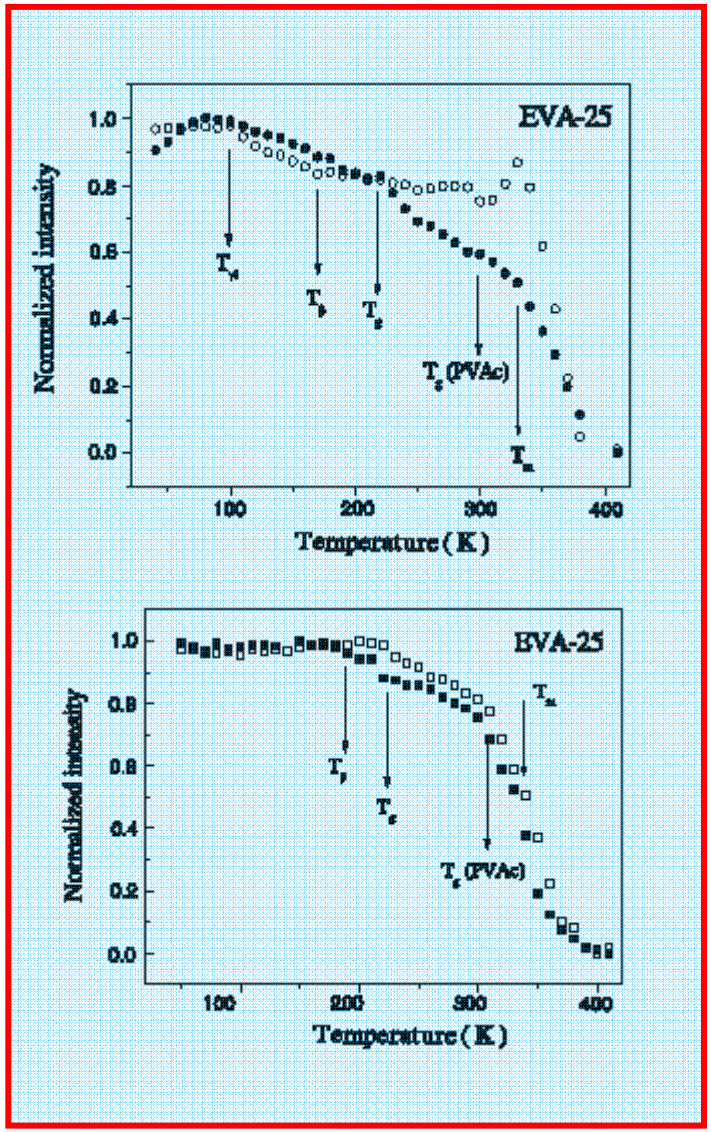

First (dark) and second (open) scans

Transition temperatures (K) for EVA from the data shown in Fig. 5

Polymer	T (K)	Assignment
EVA-9 and EVA-18	$T_{\gamma 1} = 110–130$	Motions of methylenic segments in the amorphous phase [18,19,21,32,36]
	$T_g = 220$	Glass transition of the LDPE segments [18–21,32–39]
	$T_\alpha = 270–290$	Motions of the chains in the interfacial region of the polymer matrix [18–21,40]
	$T_m = 330–340$	LDPE melting point
EVA-25	$T_\gamma = 100$	Motions of methylenic segments in the amorphous phase [18,19,21,32,36] and motions of end groups
	$T_\beta = 180–190$	Small amplitude rotary motions of one or two monomeric VAc units in an amorphous region [9,40–46]
	$T_g = 220$	Glass transition [18–21,32–39]
	T_α (PE) or T_g(VAc) = 300–310	Motions of the chains in the interfacial region of the polymer matrix [18–21,40]
	$T_m = 330–340$	LDPE melting point
EVA-33 and EVA-40	$T_\gamma = 100$	Motions of end groups
	$T_\beta = 180–190$	Small amplitude rotary motions of one or two monomeric units in an amorphous region [9,40–46]
	$T_g = 230$ K	Glass transition [18–21,32–39].
	T_g (PVAc) = 300–310	Mobility of the chains in the interfacial region of the polymer matrix [18–21,40] coupled with the PVAc glass transition [40]
	$T_m = 330–340$	LDPE melting point

Naylons = condensation of an amide a carboxylic acid

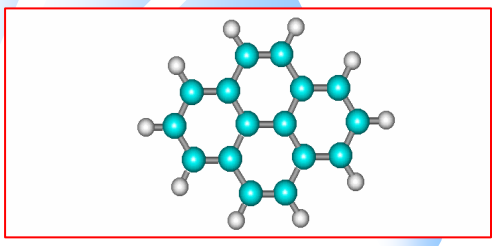

Poly(caprolactone)

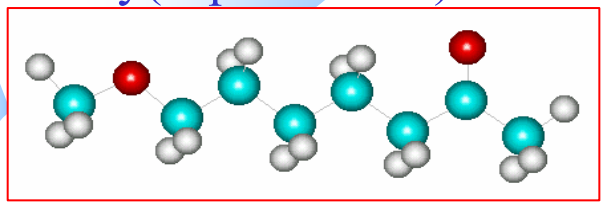

Naylon-6

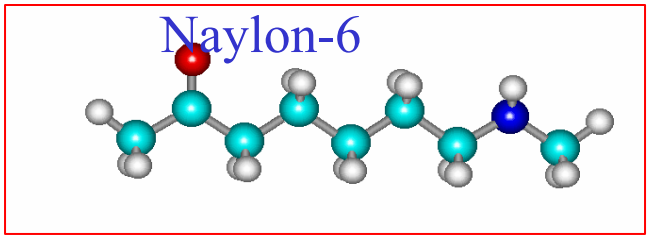

Naylon-11

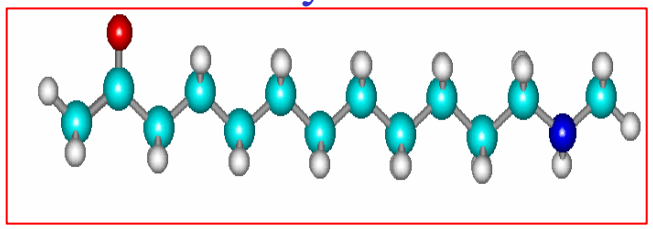

Naylon-6,6

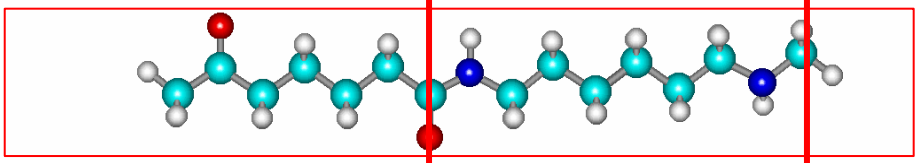

Naylon-6,9

constant

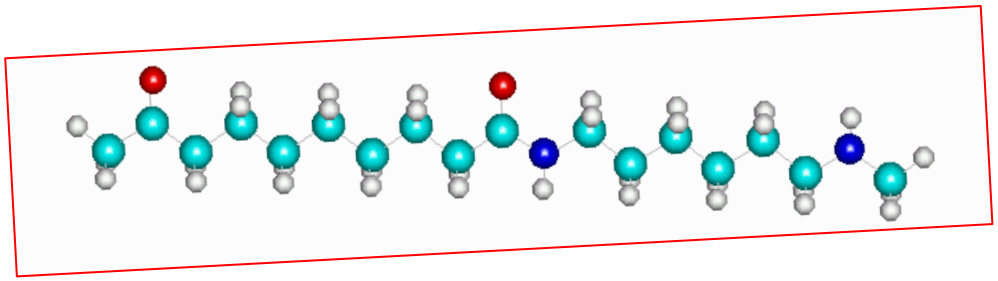

Naylon-6,10

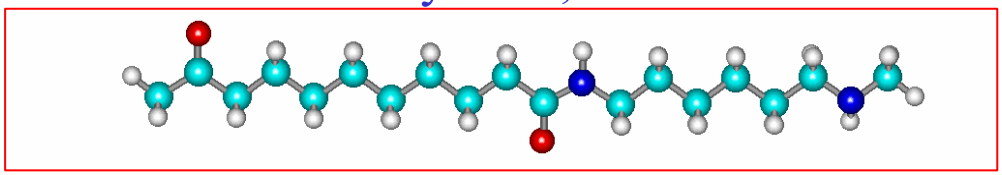

Naylon-6,12

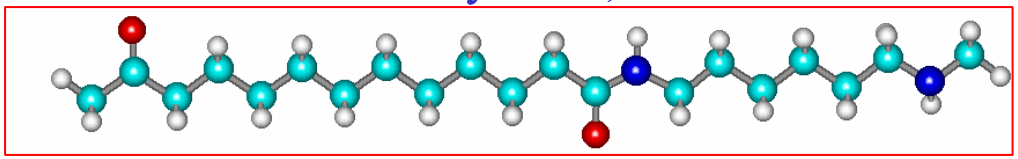

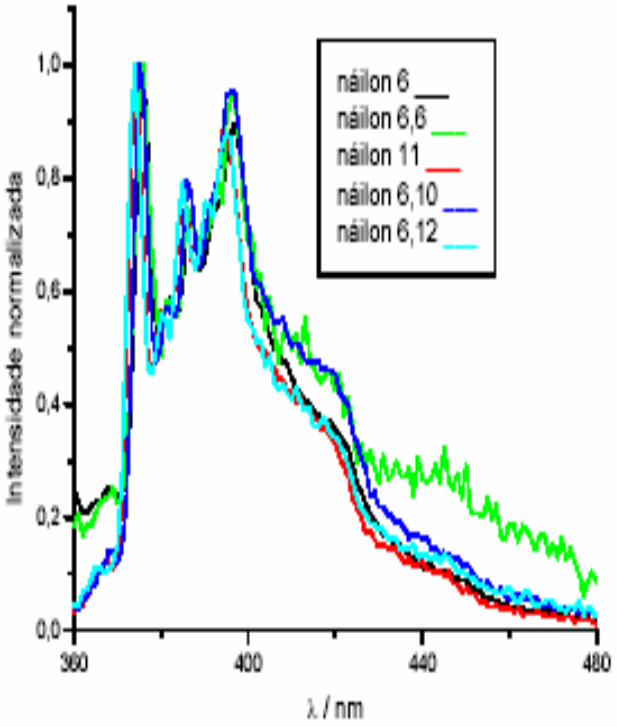

Figura 1. Espectros de fluorescência fotoestacionária do pireno em diferentes náilons. A intensidade foi normalizada em relação à banda III (385 nm).

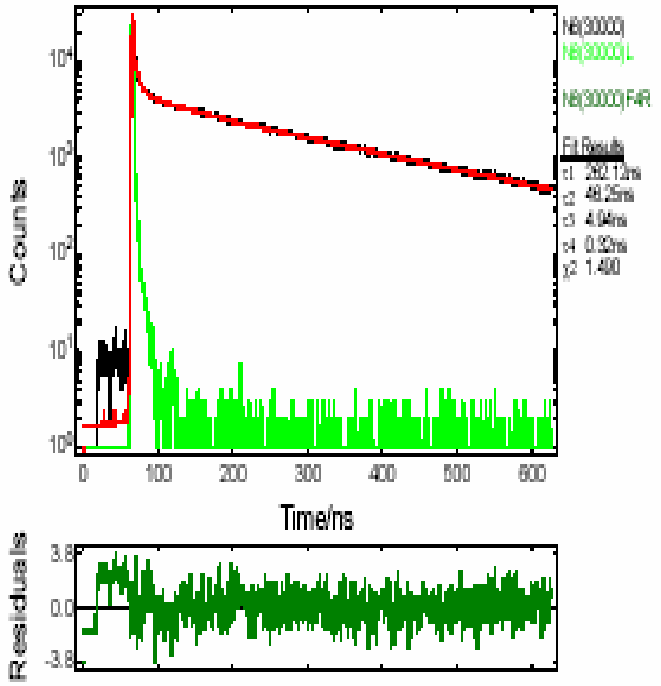

Figura 2. Curva de decaimento de fluorescência do pireno sorvido em matriz de náilon-6 (superior) e curva de distribuição de resíduos do cálculo de deconvolução em relação ao decaimento da lâmpada.

Photophysical properties of pyrene in naylons

Poly(caprolactam)	1.15	265 ns
Naylon-6	1.41	260 ns
Naylon-11	1.27	276 ns
Naylon-6,6	1.44	250 ns
Naylon-6,9	1.31	276 ns
Naylon-6,10	1.30	296 ns
Naylon-6,12	1.29	310 ns

Decrease of the polarity

Polymers modified with luminescent groups

- Will sense the environment around the molecule
- More sensivity to the motions involving the segments where they were bonded
- Selective attachment should enhance the sensitivity and coupled motions can be analyzed.

Polyethylene and vinyl acetate copolymers modified with pyrenyl groups

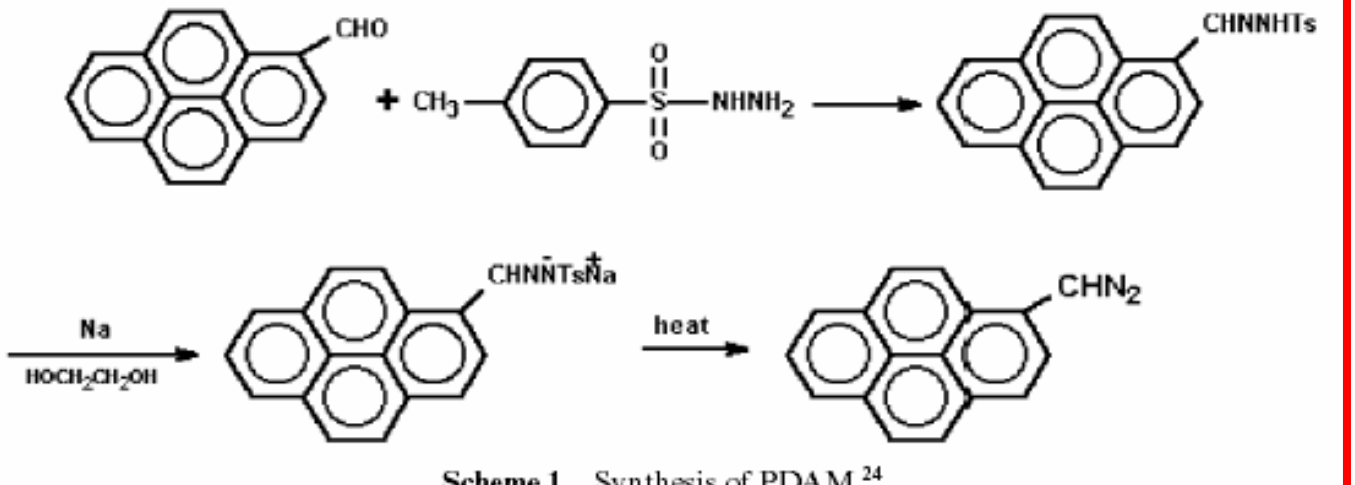

Scheme 1 Synthesis of PDAM.[24]

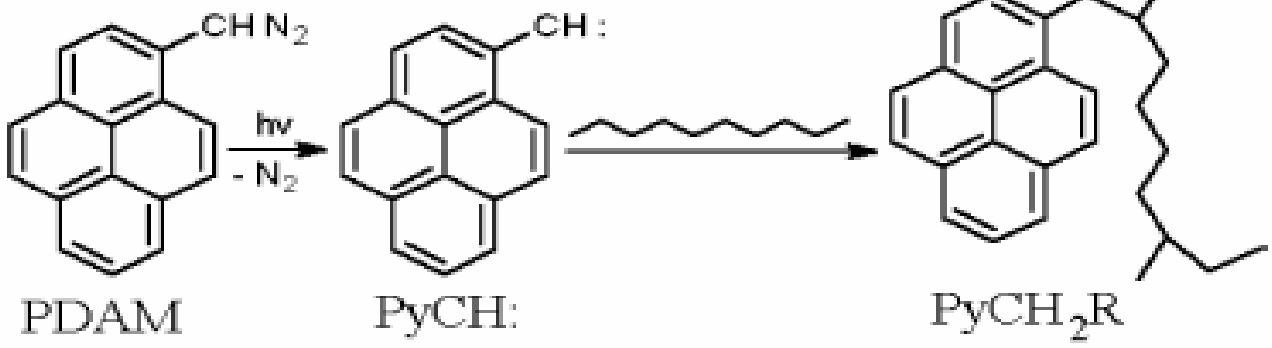

Fig. 1 Carbene insertion into 2° C–H bonds along methylene chains of polyethylene.[33] See text and Fig. 2 for other possibilities.

Weiss, et al., 1992

Selective attachment

Our results demonstrate that, regardless of the complexity of the micromorphology of EVA copolymers, selective covalent attachment of fluorescent reporters to the polymeric chains can be achieved *via* reactions with pyren-1-ylcarbene, produced photochemically *in situ*.

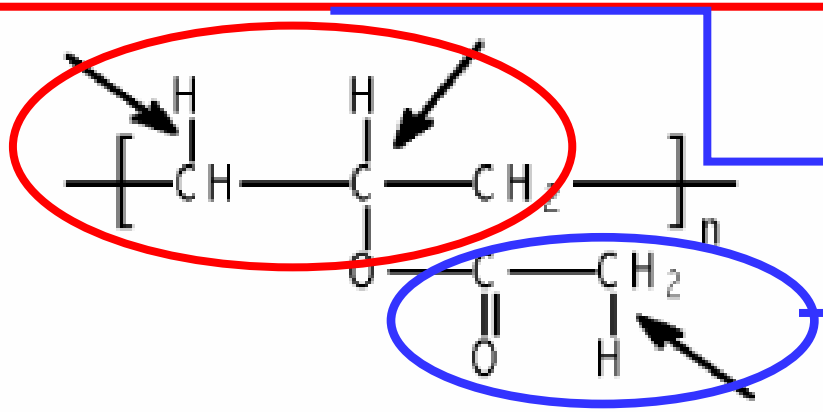

Fig. 2 Possible attachment sites for insertion of pyrenyl groups (indicated by arrows) on pendant acetate groups of EVA and PVAc polymer chains.

Relaxation processes will be associated with these groups

Not observed

Yamaki, et al., Photochem. Photobiol. Sci. 2002.

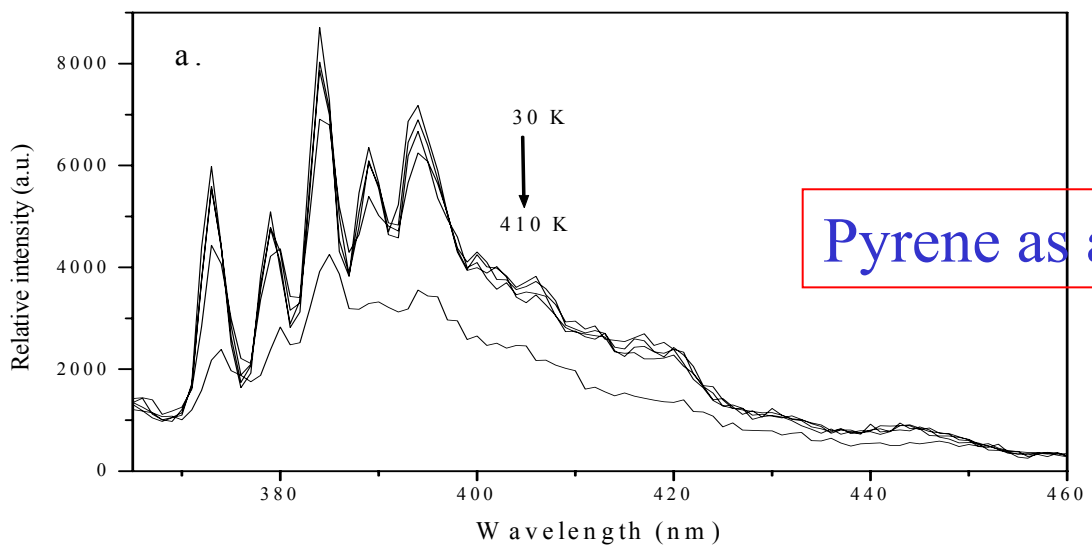

Pyrene as a guest in LDPE

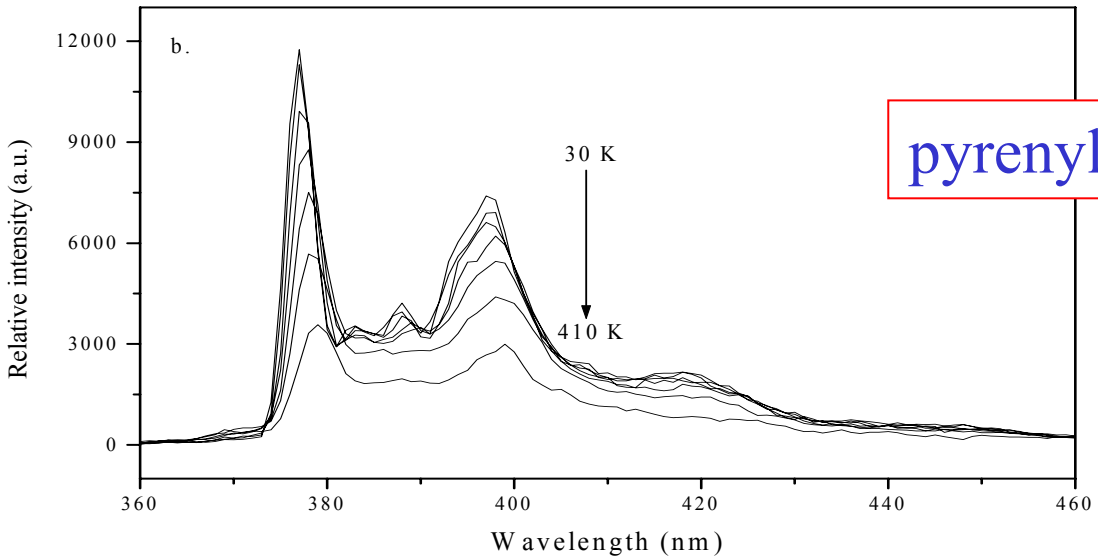

pyrenyl attached to LDPE

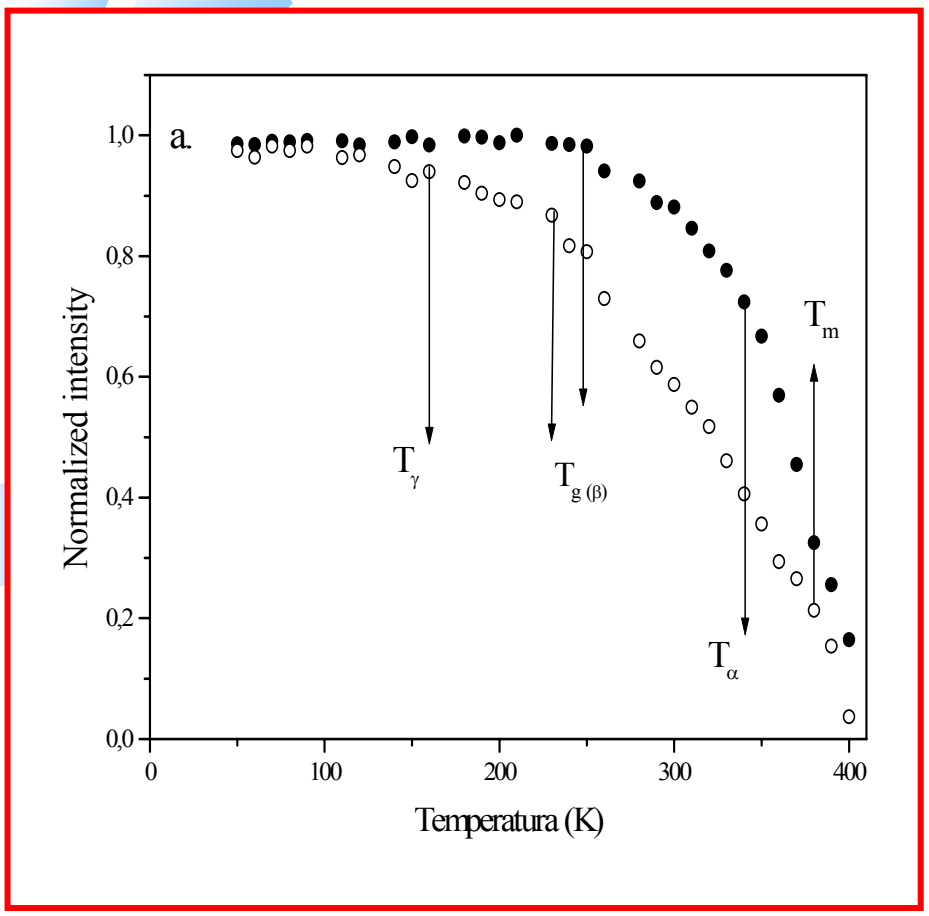

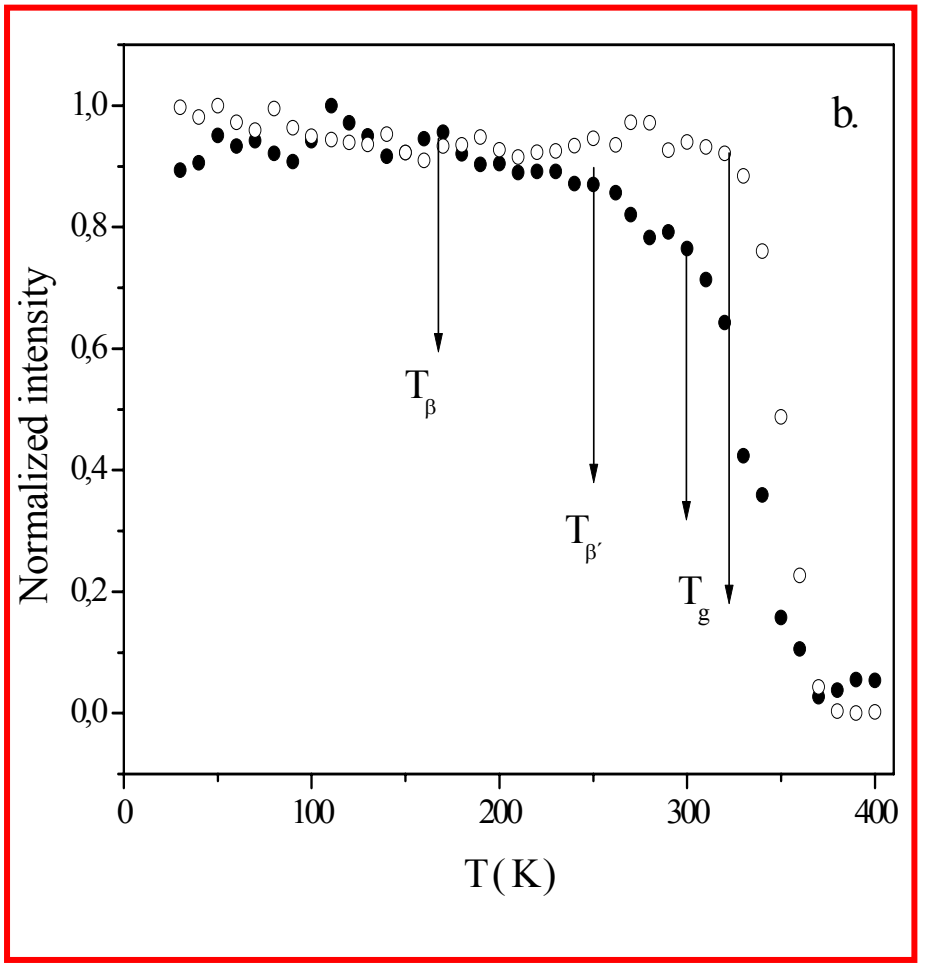

Normalized and integrated fluorescence intensities versus temperature for pyrene (●) and 1-pyrenyl groups (○) in (a) LDPE and (b) PVAC.

Scheme 1. Protocols for Covalent Attachment of 9-Anthryl (An) Groups to PE Chains; R = $AnCH_2-$ (2) and $An(CH_2)_{10}-$ (3)[11,13,24,27]

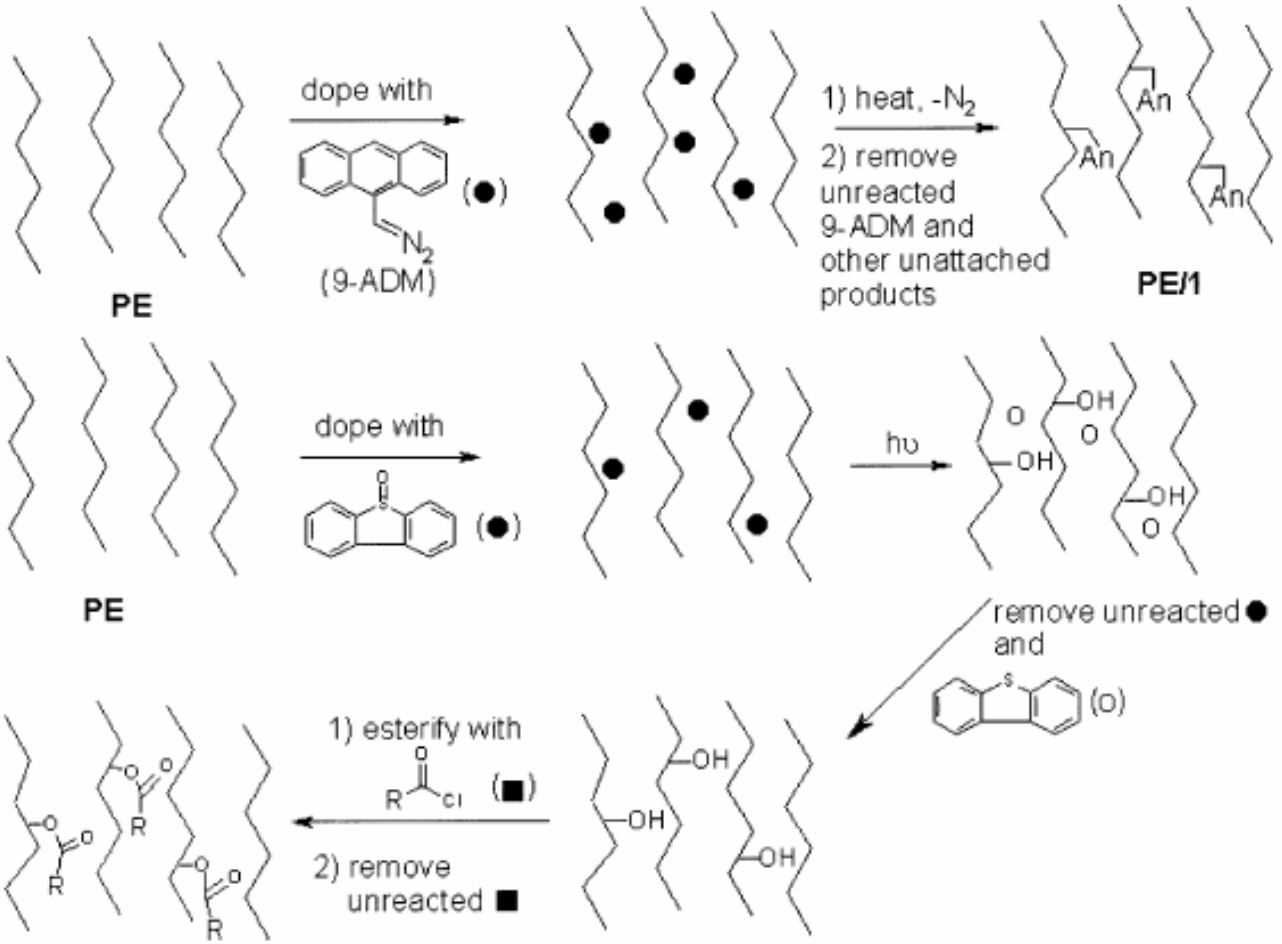

Schur, Weiss et al., Macromolecules, 2003

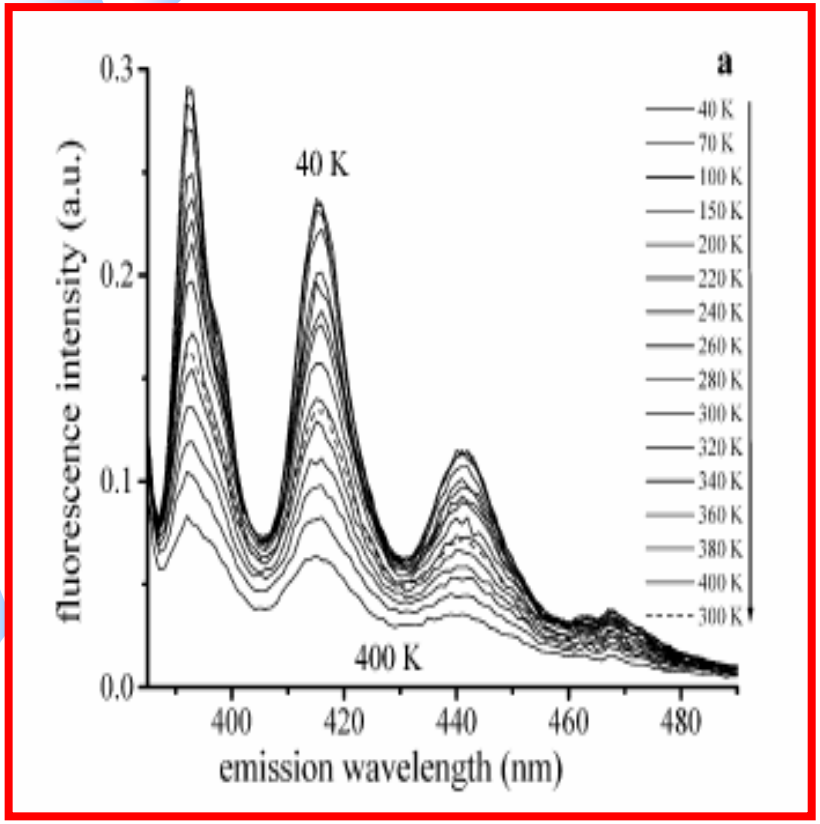

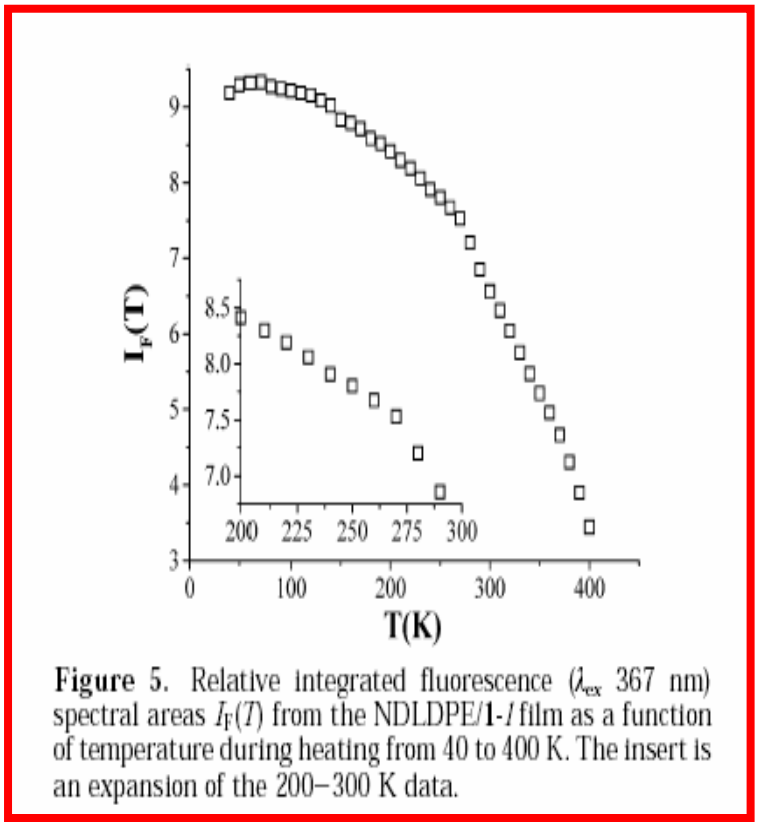

Figure 5. Relative integrated fluorescence (λ_{ex} 367 nm) spectral areas $I_F(T)$ from the NDLDPE/**1**-*1* film as a function of temperature during heating from 40 to 400 K. The insert is an expansion of the 200−300 K data.

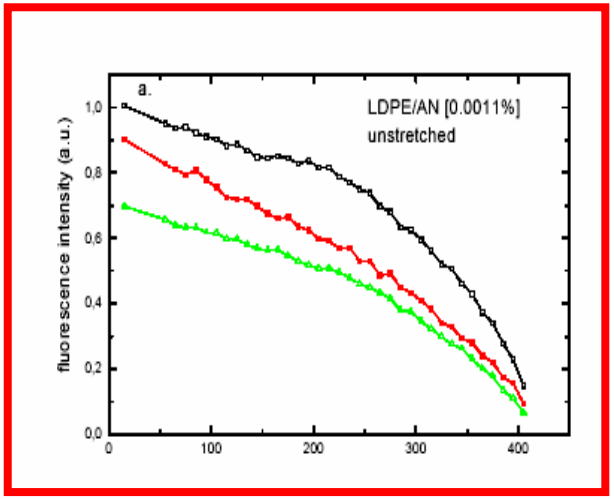

Weiss et al., Macromolecules, 2003

Intrinsically luminescent polymers: poly(2-vinyl naphthalene)

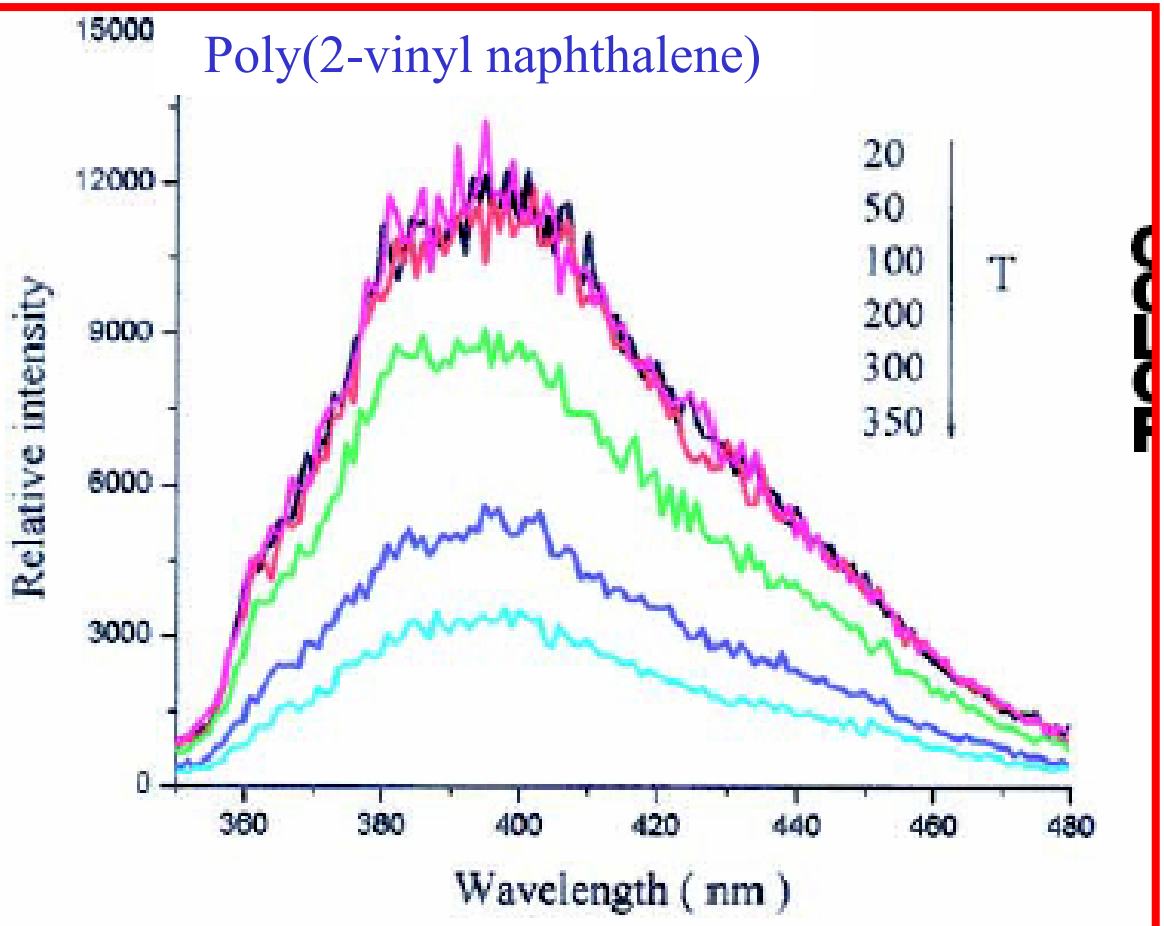

Figure 8 The typical fluorescence emission of P2VN in the solid state and in a 50/50 wt % PB-36/P2VN blend at several temperatures.

Cruz, et al. J. Appl. Polym. Sci. 2001

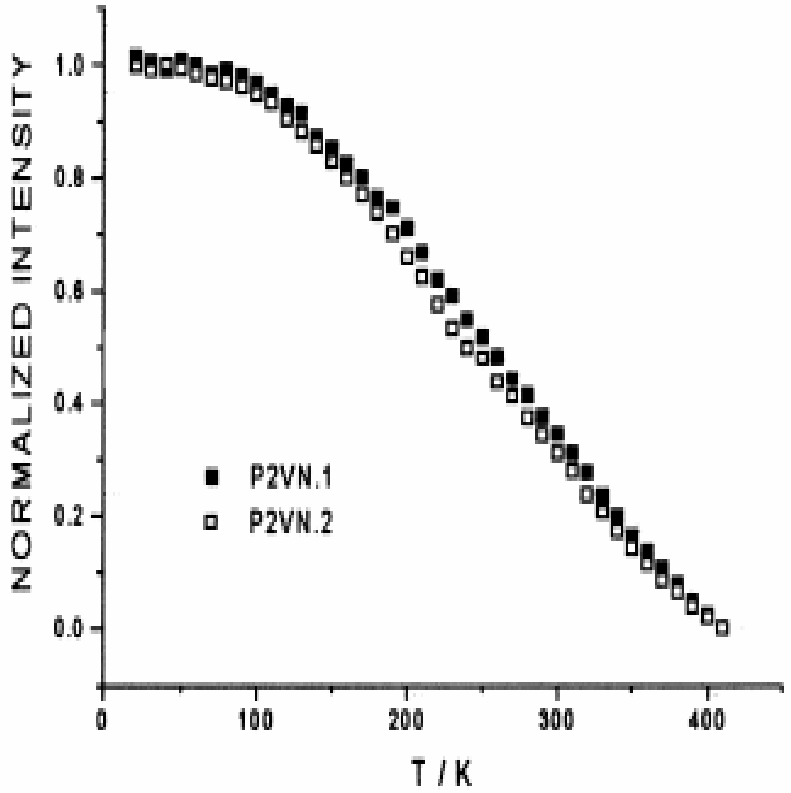

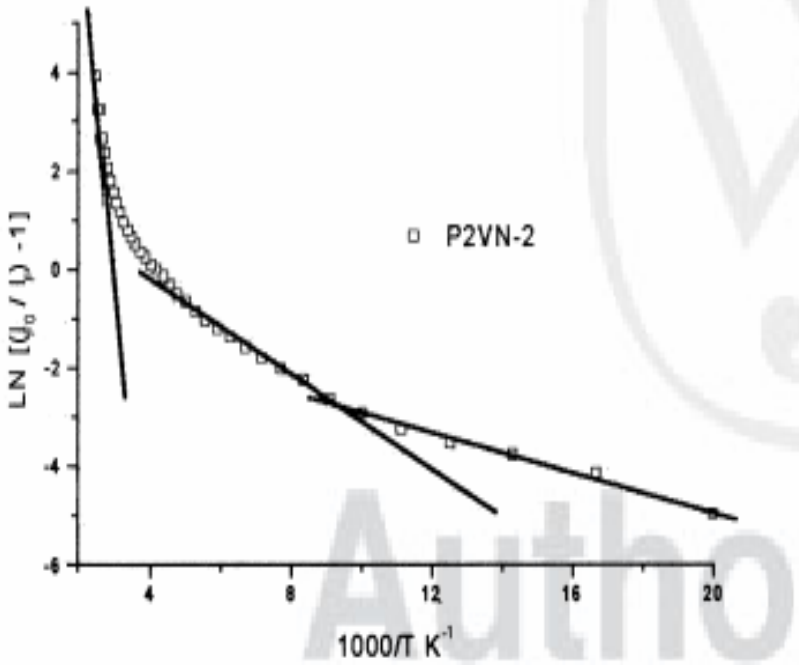

(c)

Figure 9 (a) The temperature dependence and (b,c) Arrhenius plots of the normalized and integrated fluorescence intensity of the P2VN first (-1) and second (-1) heating runs.

Table II Relaxation Temperatures and Apparent Activation Energies for P2VN by Fluorescence Spectroscopy

	P2VN-1		P2VN-2	
Assignment	T (K)	E_a (kJ mol^{-1})	T (K)	E_a (kJ mol^{-1})
γ' Relaxation	Not observed		110	1.7
γ Relaxation	200	4.2	200	3.9
T_g	370	67	370	64

T_g (P2VN) = 390 K and T_g (PB) = 187 K, both determined by DSC; 1 and 2 represent the data for the first and second runs.

Intrinsically luminescent polymers:

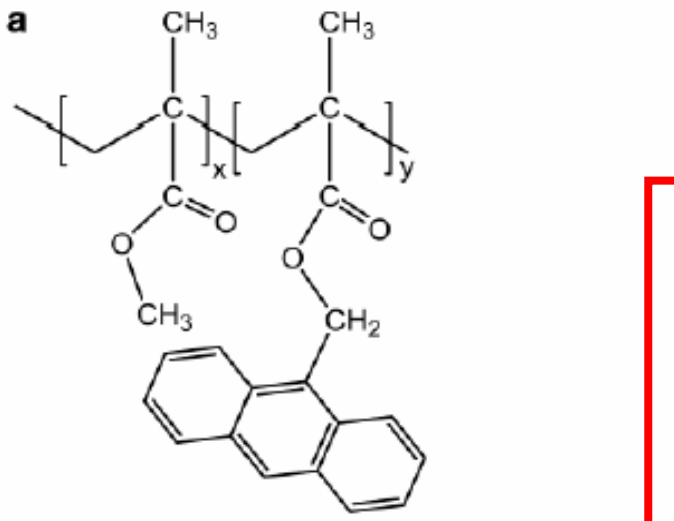

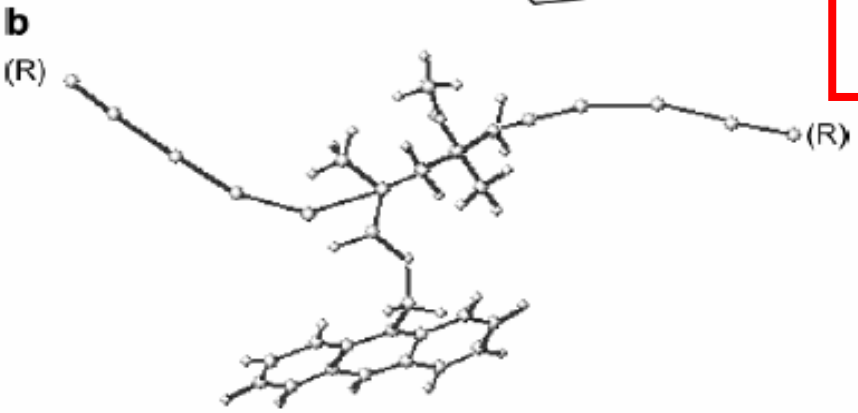

Figure 1. (a) Chemical structure of poly(MMA-*co*-MMAnt). $x = 98, 35, 25, 10, 4, 2, 0$; $y = 1$. (b) Optimized geometry of a MMA−MMAnt linkage. The (R) represents the main chain.

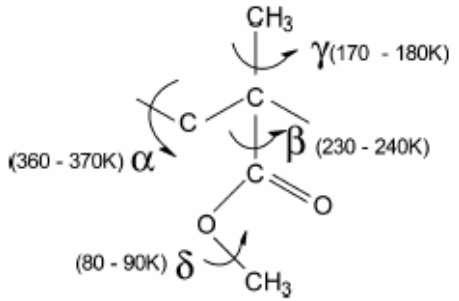

Figure 9. Illustration of the relaxations detected in PMMA through the technique of fluorescence emission with the variation of the temperature.

Deus, Akcelrud, et al. Chem. Phys. 2004

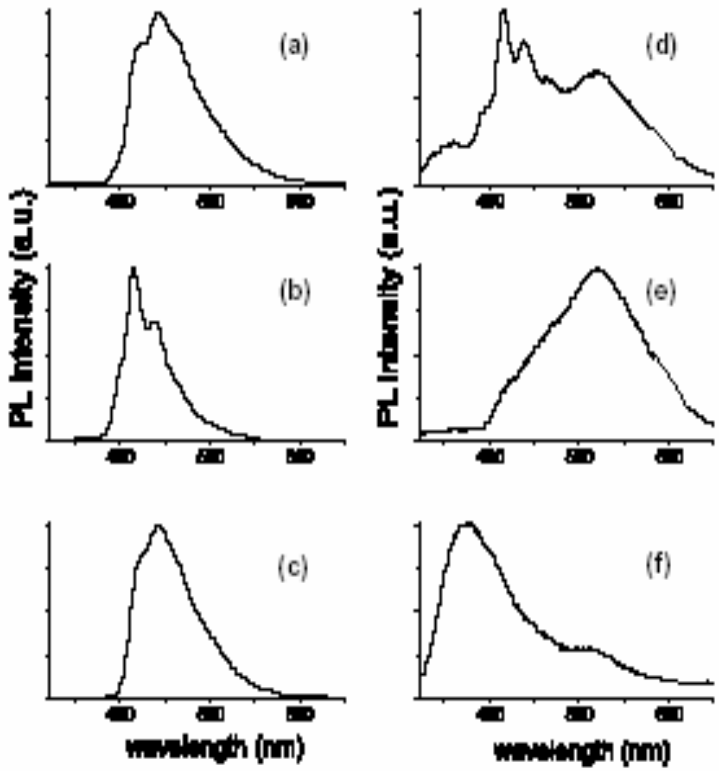

Fig. 8. Solid state fluorescence emission spectra of copolymers poly (MMA-co-MMAnt): (a) 35:1, (b) 25:1, (c) 10:1, (d) 4:1, (e) 2:1 and (f) homopolymer (PMMAnt). $\lambda_{exc} = 350$ nm.

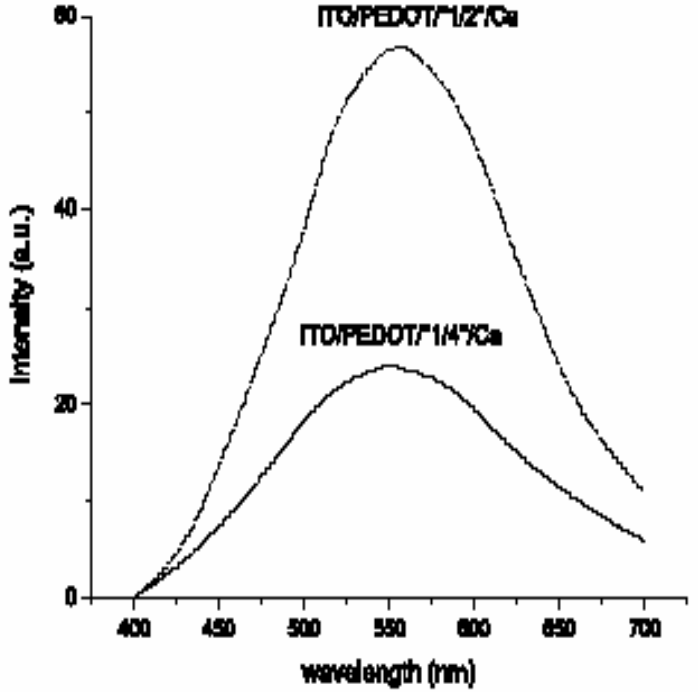

Fig. 10. Electroluminescence of copolymers 2:1 and 4:1. LED configuration: ITO/PEDOT/polymer/Ca/Al.

Deus, Akcelrud, et al. Chem. Phys. 2004

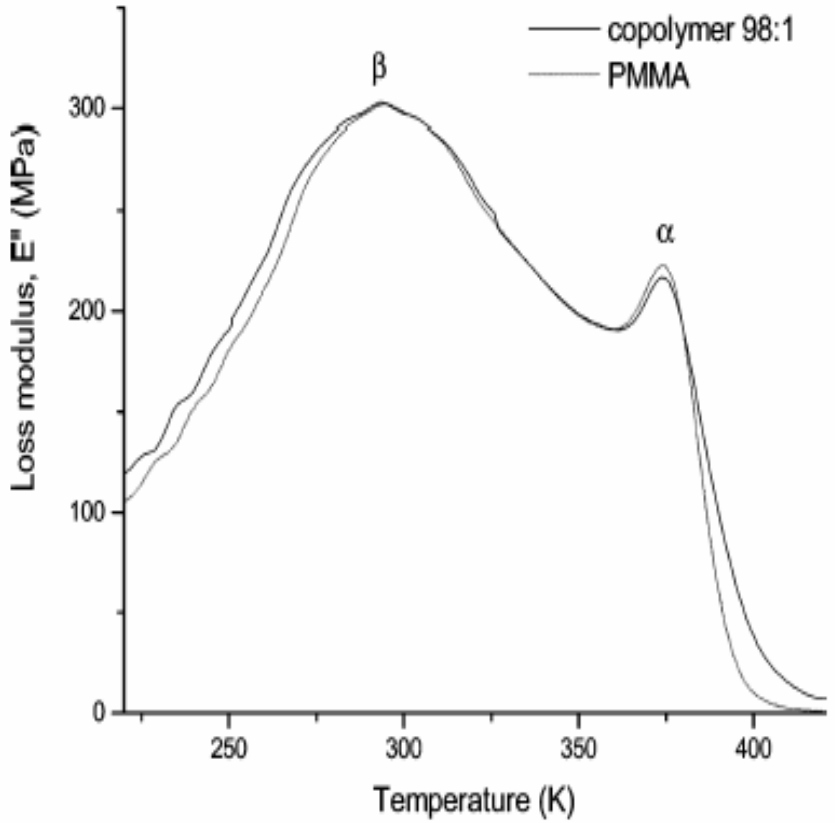

Figure 5. Temperature dependence of loss modulus (E'') for poly(methyl methacrylate) and poly(methyl methacrylate-*co*-9-methylanthryl methacrylate) (98:1). Frequency = 3.3 Hz.

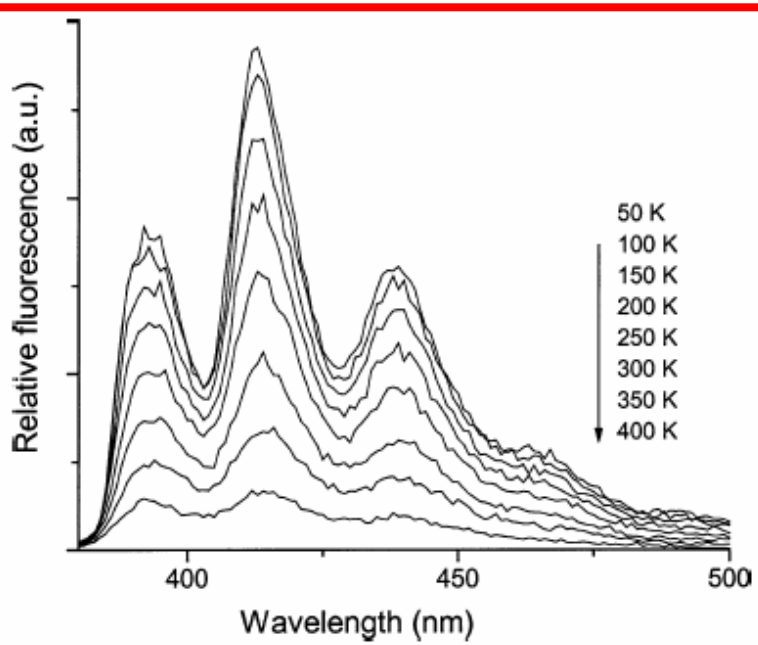

Figure 6. Fluorescence spectra of the probe (anthryl group) in poly(methyl methacrylate-*co*-9-methylanthryl methacrylate) (98:1) at several temperatures.

Deus, Akcelrud, et al. Macromolecules 2004

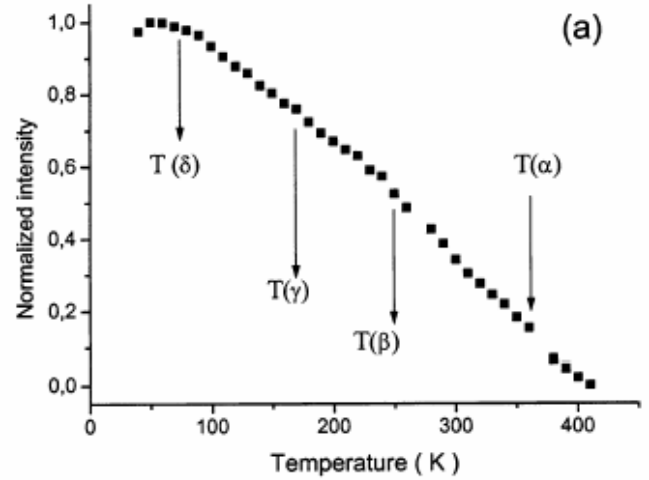

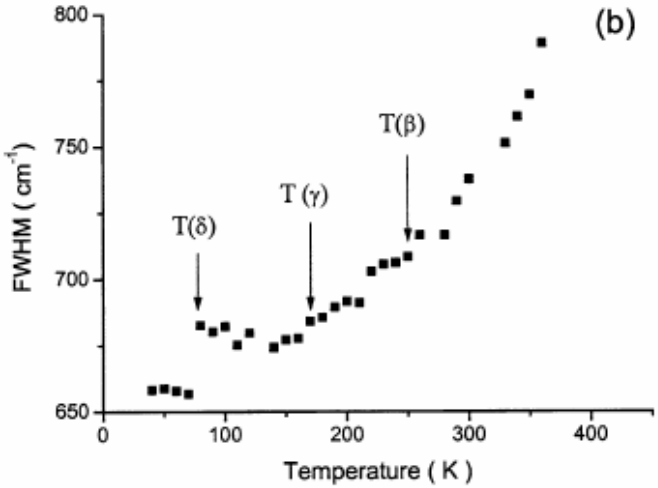

Figure 7. (a) Integrated and normalized fluorescence intensities for poly(methyl methacrylate-*co*-9-methylanthryl methacrylate) (98:1 molar ratio) vs temperature. (b) Full width at half-maximum (FWHM) of the 0−0 band at the same temperature range.

Relaxations of Poly(methyl methacrylate) E

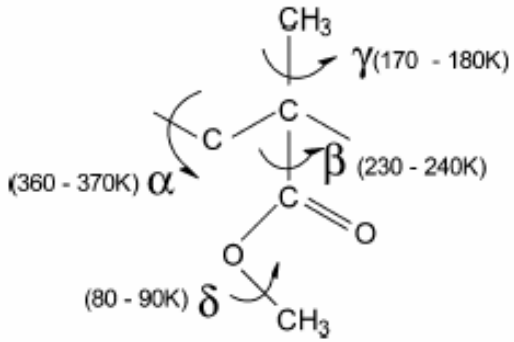

Figure 9. Illustration of the relaxations detected in PMMA through the technique of fluorescence emission with the variation of the temperature.

Conjugated luminescent polymers

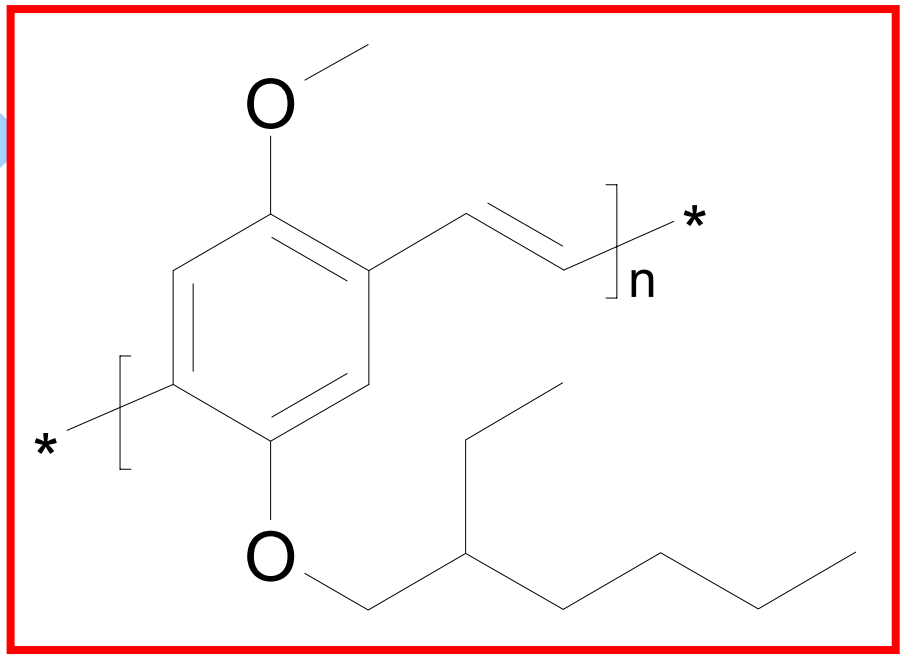

Poly(2-methoxy-5-(2-ethylhexyloxy)-p-phenylene vinylene)

MEH-PPV

ady-state
orescence
ission

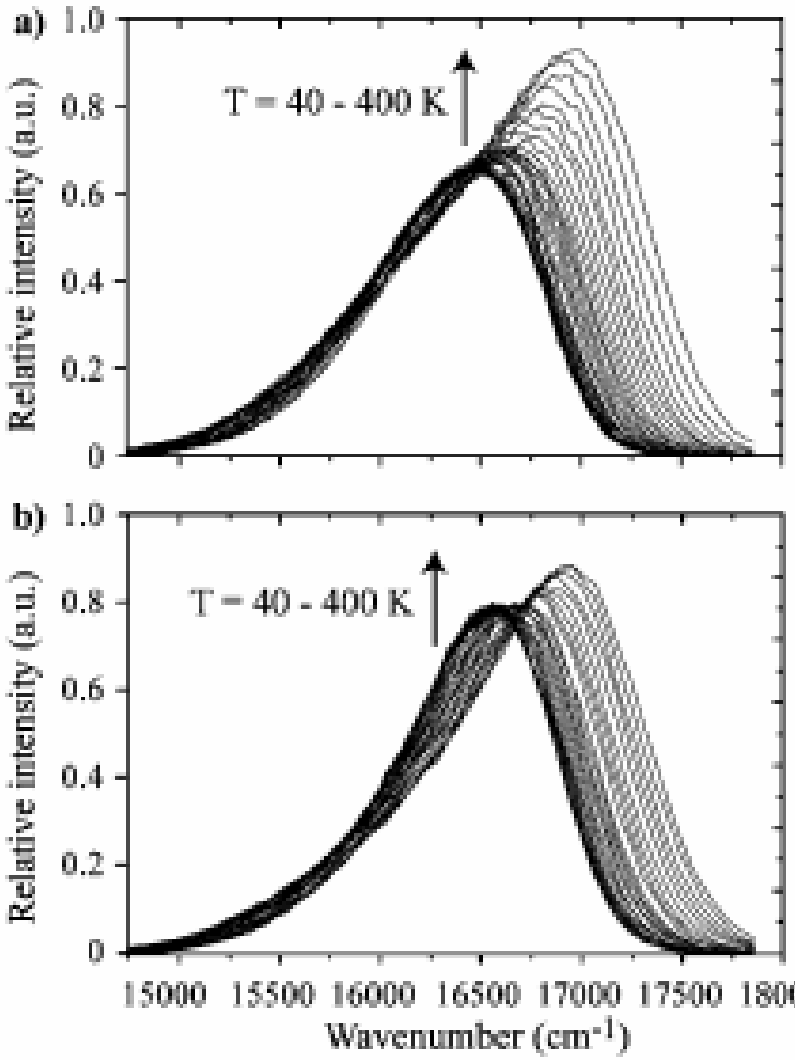

Figure 1. Photoluminescence spectra at several temperature (from 40 to 400 K) for MEH–PPV spin-coated films: (a) spu from chloroform; (b) spun from toluene. λ_{exc} = 21 270 cm^{-1}.

Blue shift

Increase of intensity

Cossiello, et al. Macromolecules 2005

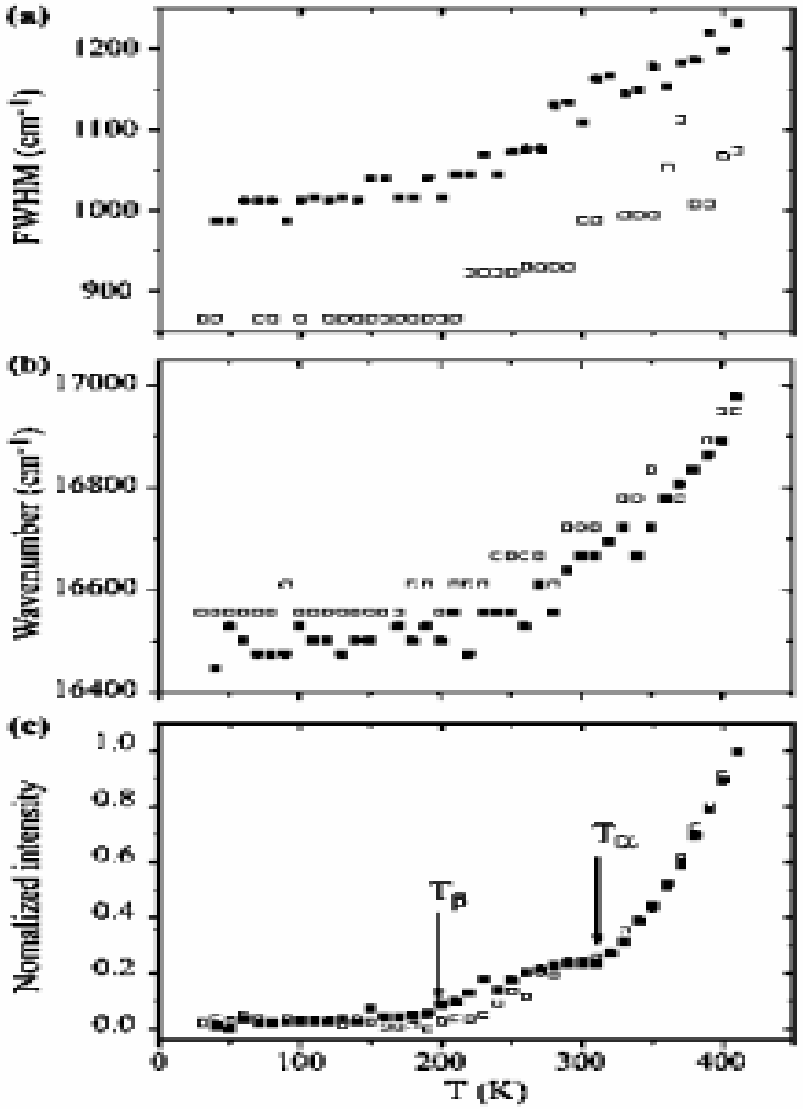

Figure 2. (a) Fwhm, (b) photoluminescence peak maxima (cm^{-1}), and (c) integrated and normalized intensity, $I_F(T)/I_F(T_0)$, at several temperatures for MEH−PPV films: spun from toluene (□) or spun from chloroform (■). $\lambda_{exc} = 21\ 270\ cm^{-1}$.

DMTA data

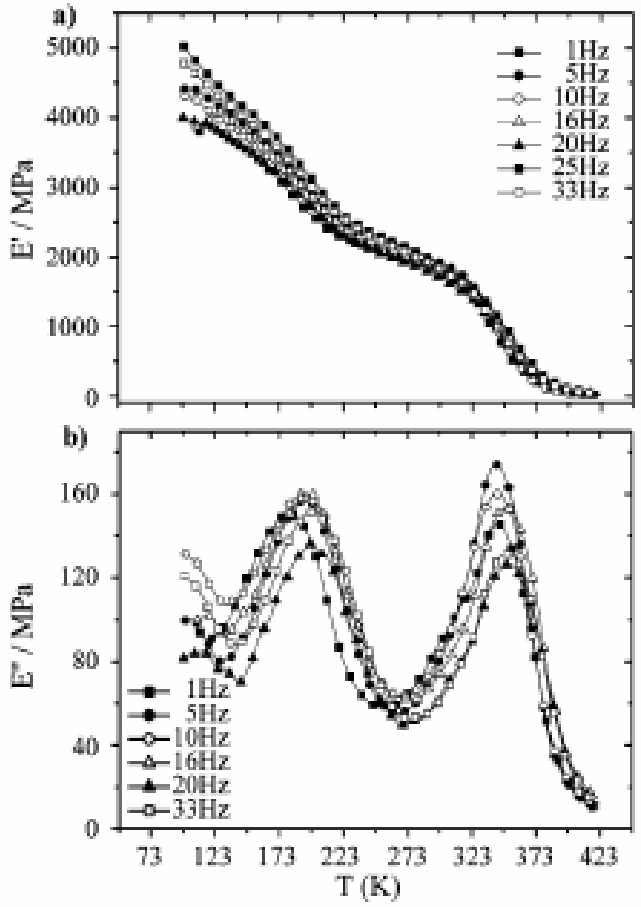

Figure 5. DMTA plots for a film of MEH–PPV at several frequencies.

Arrhenius plots

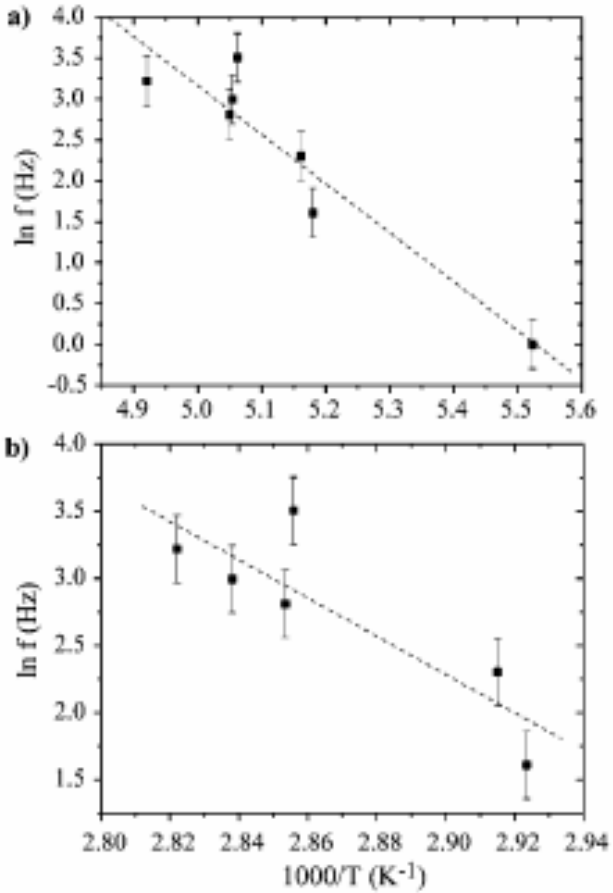

Figure 6. Arrhenius plots for the β (a) and α (b) relaxations by DMTA.

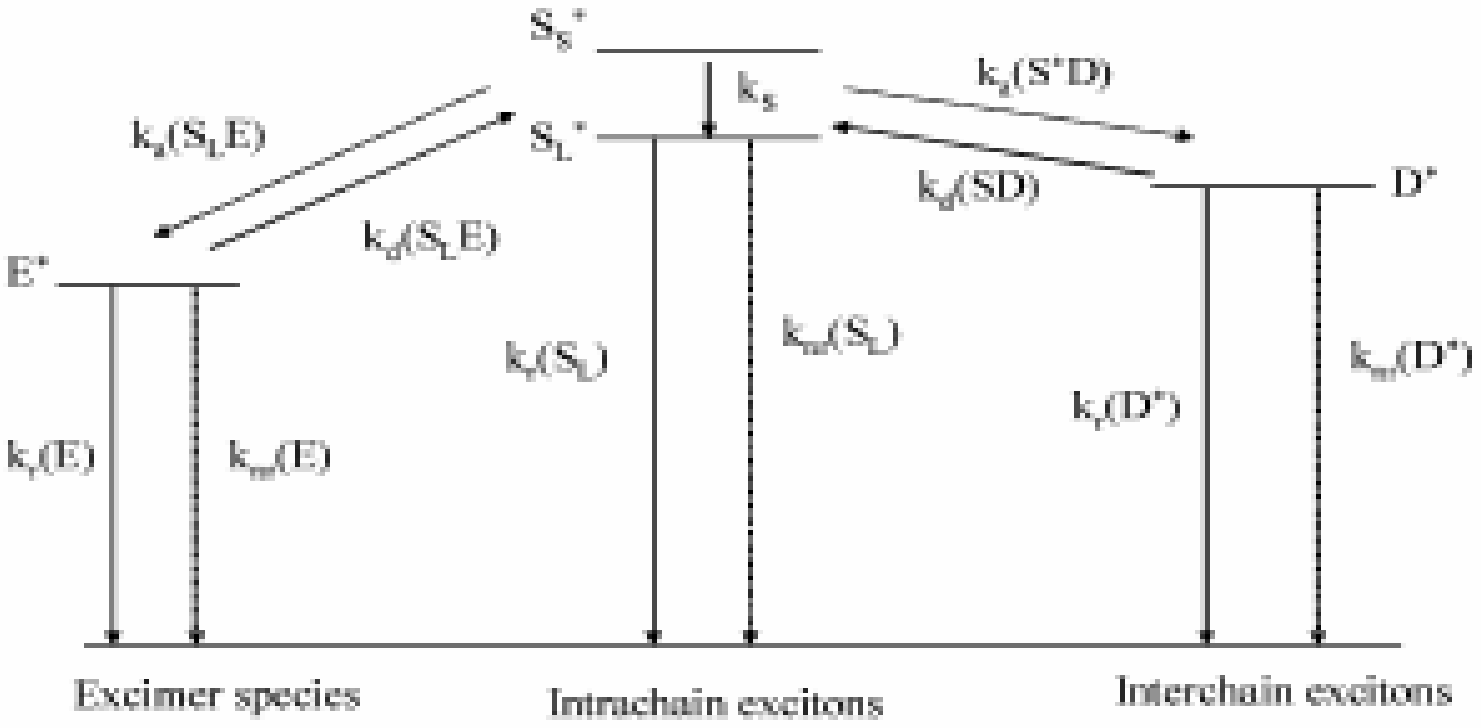

Figure 3. Kinetic scheme for the fluorescence decays of MEH–PPV films, where M is the ground-state chromophore, M* is an excited-state species, I is the intrachain exciton, D* is the excited-state aggregate, k_{nr} and k_r are the radiationless and radiative rate constants, respectively, $k_a(S^*_LD)$ is the rate constant for the intrachain exciton forming an excited dimer, and $k_d(S^*_LD)$ is the rate constant for the aggregated dissociation re-forming the intrachain exciton.

Relaxation processes

Techniques	β-relaxation	α-relaxation
DMTA	**T = 210 ± 10 K** **Ea = 29.1 kJ mol^{-1} K^{-1}**	**T = 330 ± 10 K** **Ea = 85.4 kJ mol^{-1} K^{-1}**
TSC	**T = 210 ± 10 K** **Ea = 22.5 kJ mol^{-1} K^{-1}**	**T = 310 ± 10 K** **Ea = 62.4 kJ mol^{-1} K^{-1}**
Fluorescence	**T = 220 ± 10 K**	**T = 320 ± 10 K**

Cossiello et al. Macromolecules, 2005

Molecular Motions by ^{13}C NMR

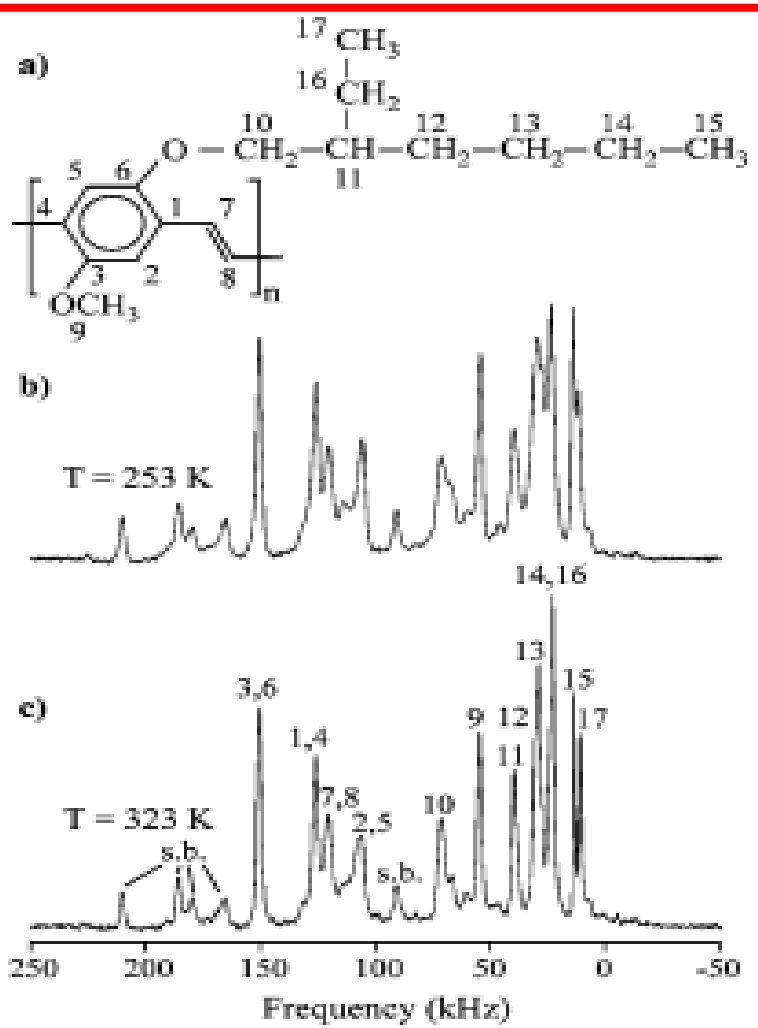

Figure 8. MEH–PPV repetitive unit (a) and magic-angle-spinning NMR spectra of MEH–PPV with the corresponding line assignments at (b) 253 and (c) 323 K.

Bloise, et. al. Phys. Rev. B. 2005

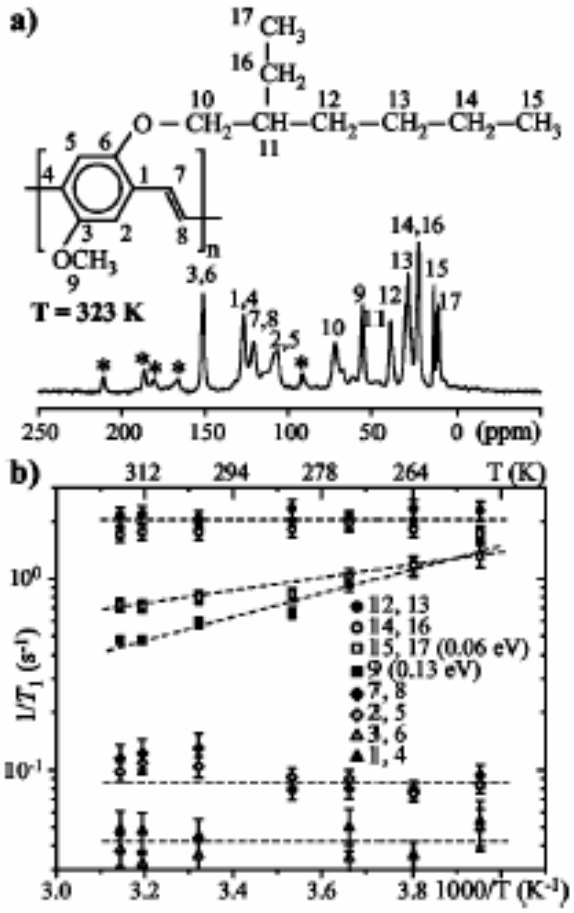

FIG. 1. (a) ^{13}C CP/MAS NMR spectra of MEH-PPV (* indicates the spinning side bands). (b) Temperature dependence of the ^{13}C spin-lattice relaxation rates (T_1^{-1}) for all the carbons of MEH-PPV.

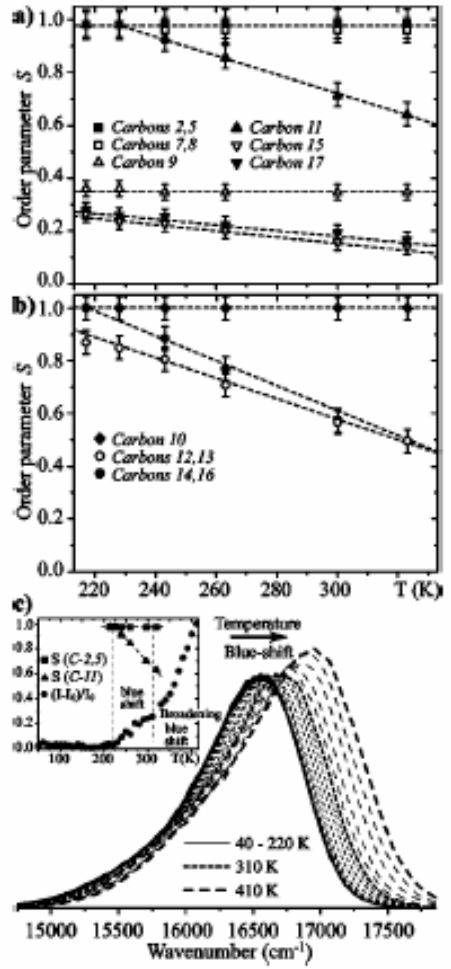

FIG. 2. (a) Plot of the molecular order parameters as a function of temperature for CH and CH_3 groups in MEH-PPV. (b) Same as in (a) for CH_2 groups. (c) MEH-PPV PL spectra at several temperatures (from 40 to 410 K). The inset shows the correlation between the differential normalized PL intensities and order parameters at several temperatures.

Bloise et al. Phys. Rev. B, 2005

Conclusions from 13C RMN

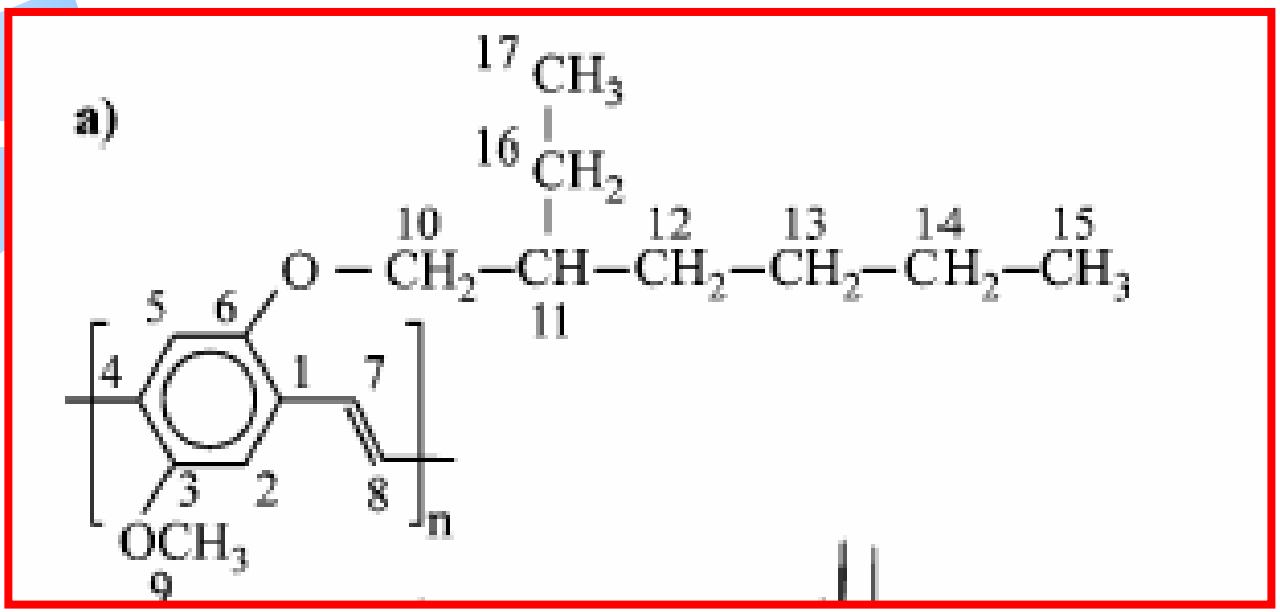

Carbons 11, 12, 13, 14, 15, 16, and 17 gain mobility after the β-relaxation process

Nanorheological approach for characterization of electroluminescent polymer thin films

Tomoko Gray, Cynthia Buenviaje, and René M. Overney[a)]
Department of Chemical Engineering, University of Washington, Seattle, Washington 98195-1750

Samson A. Jenekhe
Department of Chemical Engineering and Department of Chemistry, University of Washington, Seattle, Washington 98195-1750

Lixin Zheng and Alex K. Y. Jen
Department of Material Science and Engineering, University of Washington, Seattle, Washington 98195

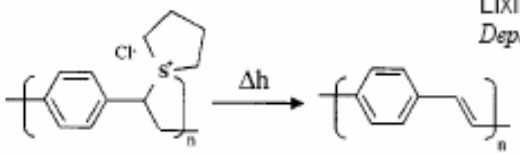

(a)

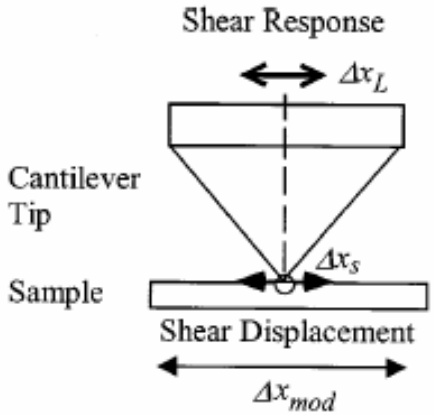

(b)

FIG. 1. (a) Thermal conversion of PPV from its sulfonium precursor. (b) Schematic of the SM-SFM. The sample is sinusoidally modulated (Δx_{mod}) relative to the probing cantilever tip. The shear response (Δx_L) is a qualitative measure of the contact stiffness (a convoluted expression of the combined shear modulus and the contact area). The contact stiffness is represented by the sample deformation Δx_S, and is directly obtained by the cantilever response Δx_L, with $\Delta x_{mod} = \Delta x_L + \Delta x_S$.

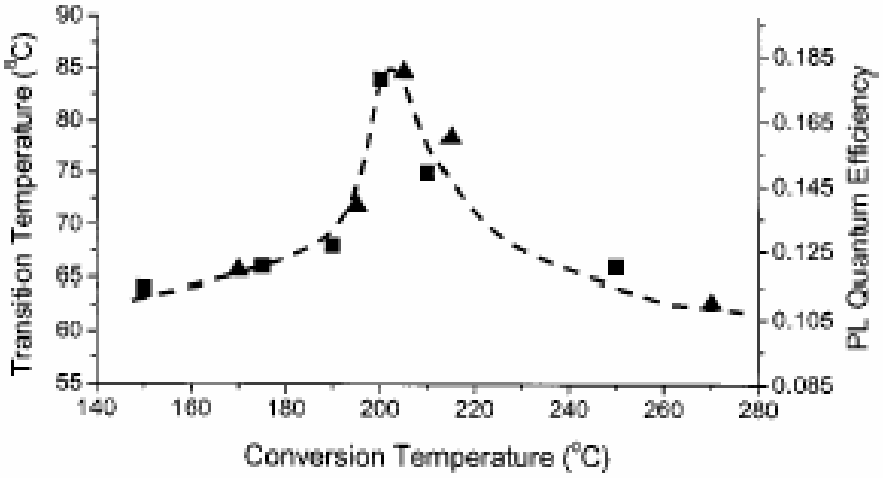

FIG. 3. Qualitative comparison of the PL efficiency (▲) (see Ref. 7) with the rheological transition (■) as function of the PPV conversion temperature. The rheological transitions were measured with the SM-SFM method. A dashed line has been added for trend enhancement.

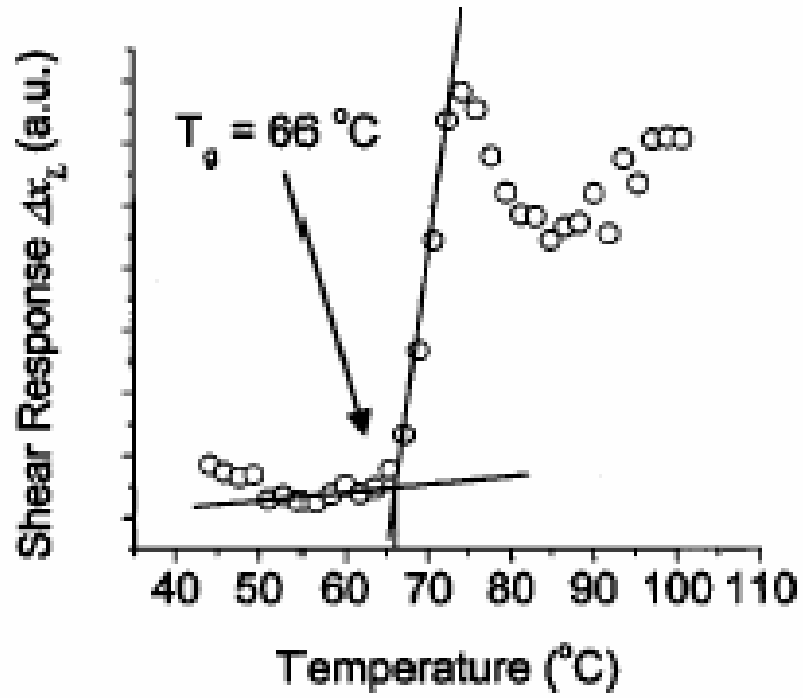

FIG. 2. Representative thermal–rheological SM-SFM plot of PPV at a conversion temperature T_{conv} of 175 °C. At T_g, the contact area increase dominates the modulus decrease of the polymer. Thus, the contact stiffness increases above T_g until the transition process is complete.

Implications of the relaxation processes on the electroluminescence properties

ELSEVIER

Synthetic Metals 111–112 (2000) 381–384

www.elsevier.com/locate/synmet

Temperature-dependent device model for polymer light-emitting diodes: significance of barrier height

J.M. Lupton *, I.D.W. Samuel

Department of Physics, University of Durham, South Road, Durham DH1 3LE, UK

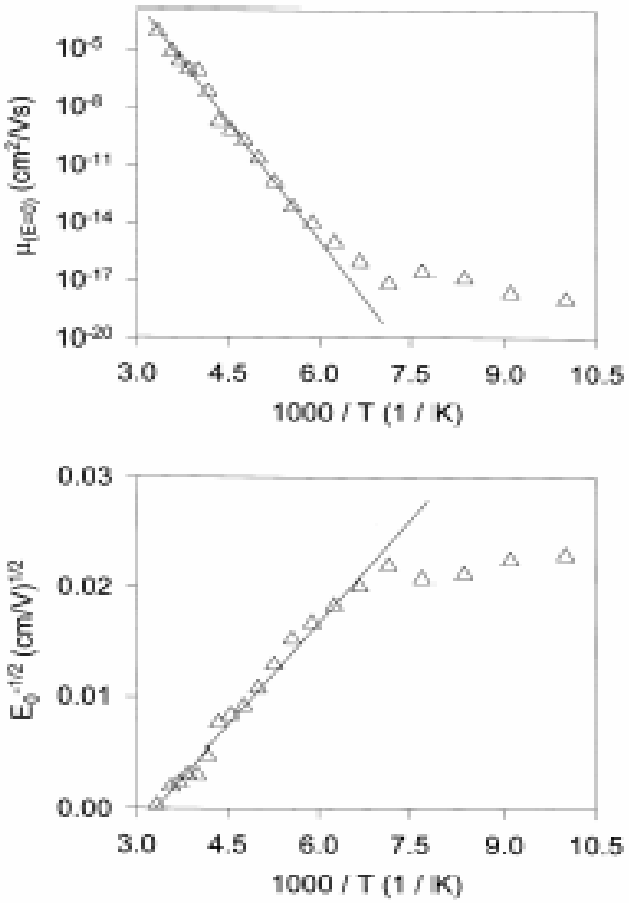

Fig. 2. Variation of the mobility parameters with temperature.

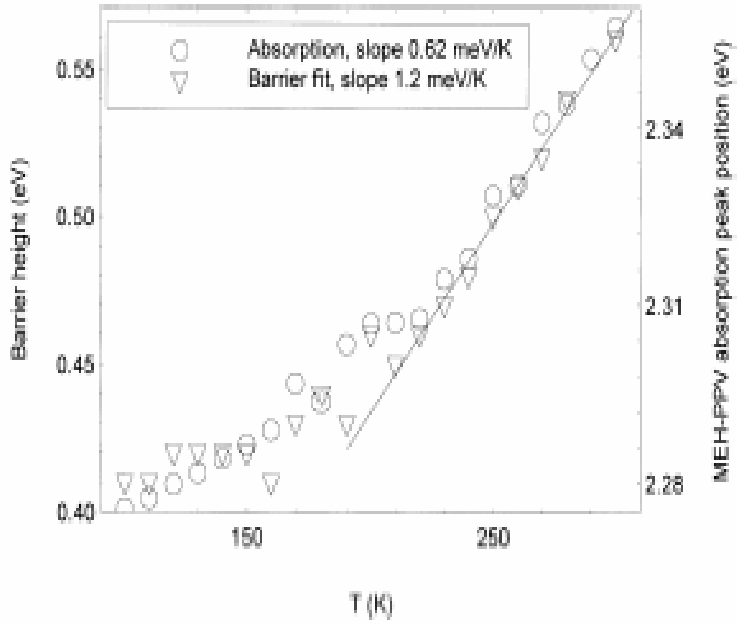

Fig. 3. Decrease of barrier height for hole injection with temperature compared to the red-shift of the absorption of MEH-PPV.

Electroluminescence and photoluminescence

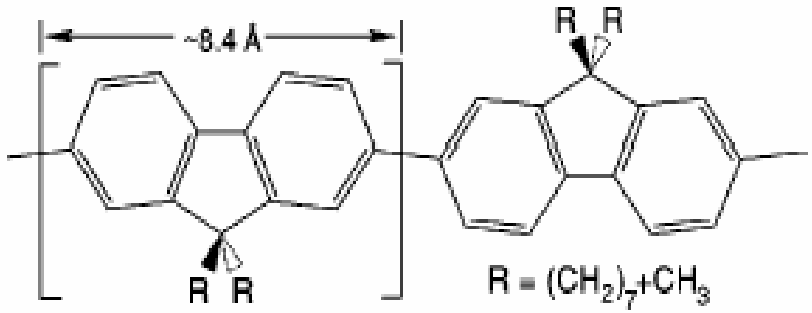

poly(9,9-(di-*n*,*n*-octyl-fluorene))

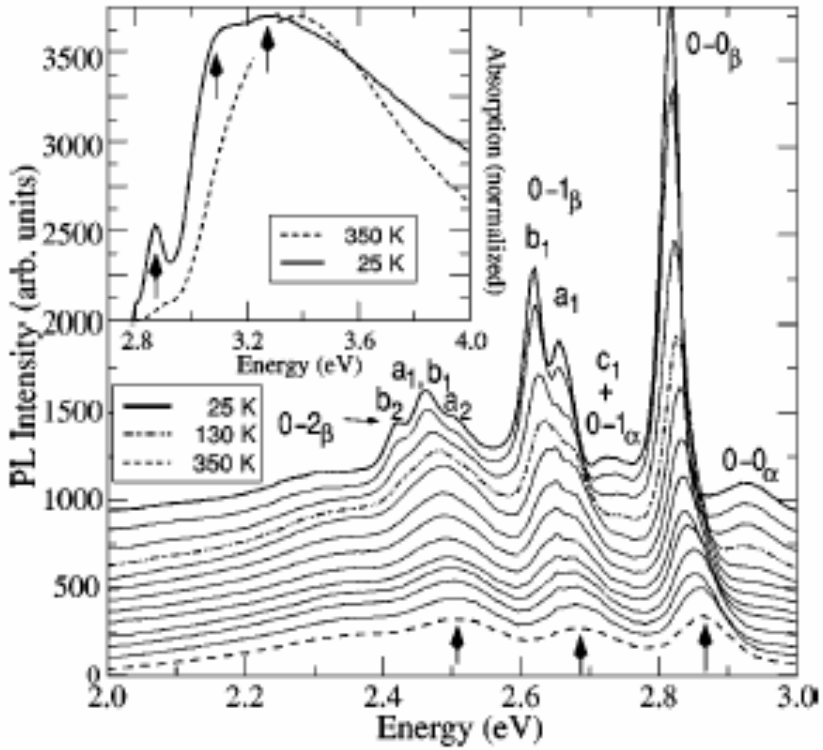

FIG. 2. Progression of PF8 sample *A* photoluminescence spectra on cooling from 350 K (λ_{Ex}=390 nm). All PL curves are self-absorption corrected and offset for clarity. Inset: Two corresponding absorption spectra with arrows indicating the β-phase 0-0, 0-1, and 0-2 vibronic bands.

Winokur et al. Phys. Rev. B. 2003

Spectral profiles and condensed medium

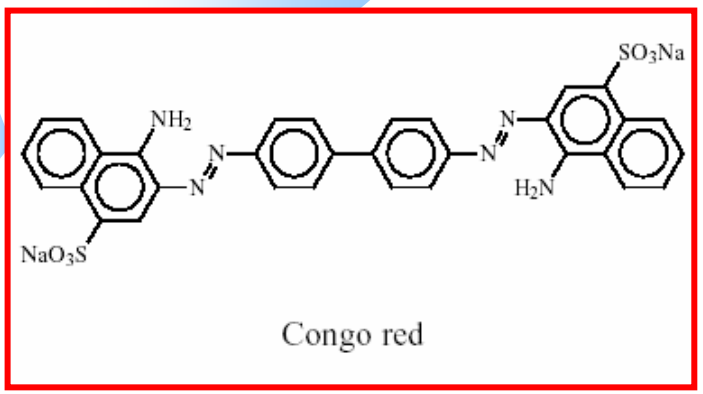

Congo red

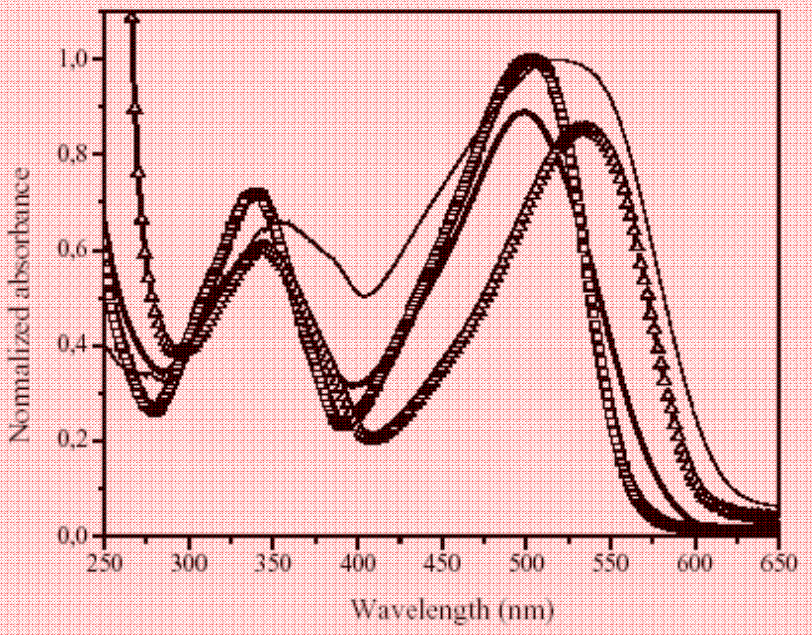

Figure 2. Electronic absorption spectra of 10^{-5} mol L^{-1} solutions (by transmittance) of CR (▬) in deionized water, (–□–□–) MeOH, (–Δ–Δ–) DMSO and (▬) CR adsorbed on cellulose fibers (by diffuse reflectance).

Spectral profiles and condensed medium

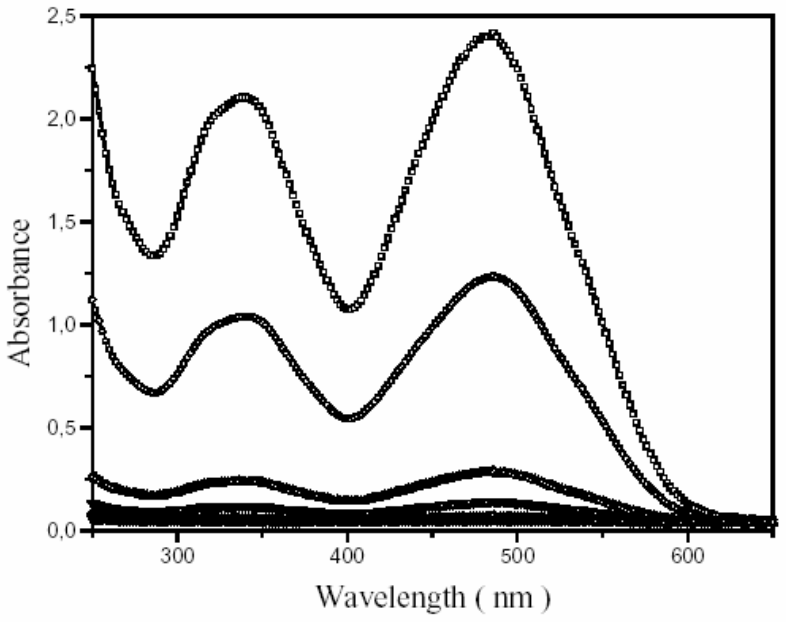

Figure 3. a. Electronic absorption spectra CR in aqueous solution of CR: (–*–*–) 7.2 10^{-6} m (–◊–◊–) 1.4 10^{-5} mol L^{-1}, (–∇–∇–.) 7.2 10^{-5} mol L^{-1}, (–Δ–Δ–) 1.4 10^{-4} mol L^{-1}, (–o–o–) 7.2 10^{-4} n and (–□–□–) 1.4 10^{-3} mol L^{-1}.

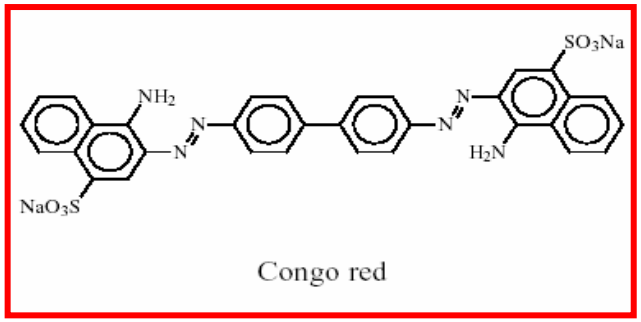

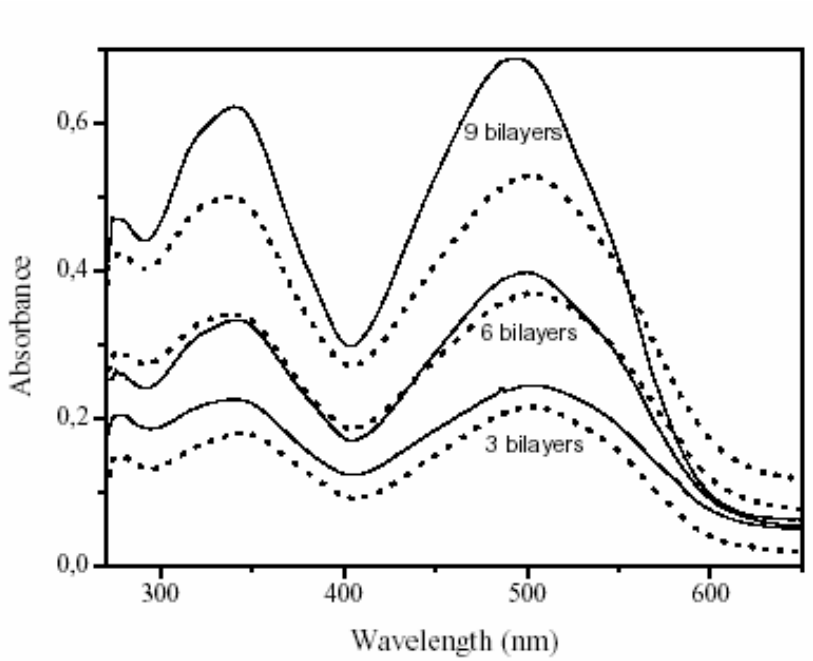

Figure 4. Electronic absorption spectra of CR/PAH LbL films prepared using dipping solution with (---) pH 2.0 and (—) pH 10.0.

Spectral profiles and condensed medium

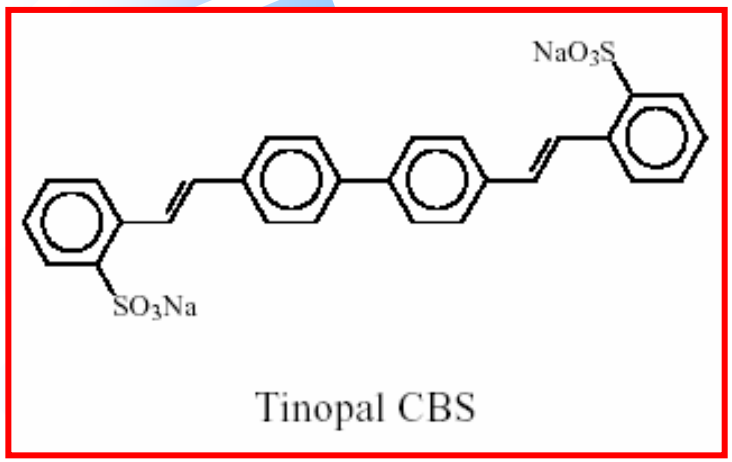

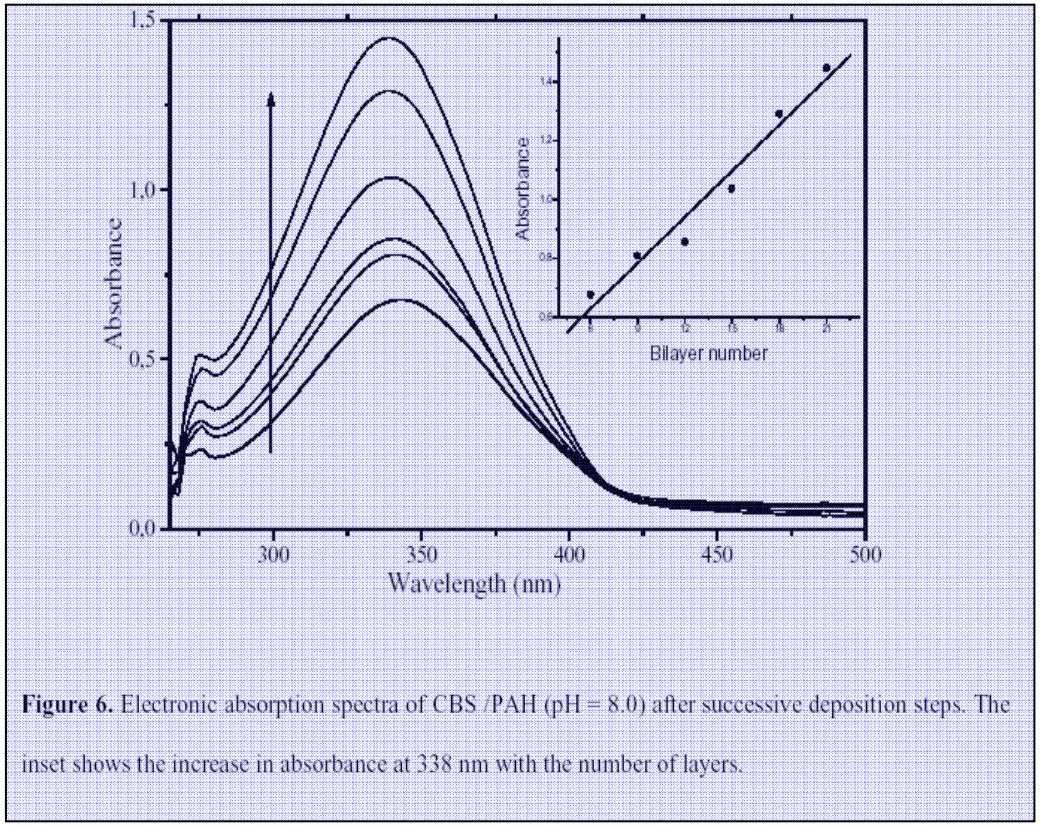

Figure 6. Electronic absorption spectra of CBS /PAH (pH = 8.0) after successive deposition steps. The inset shows the increase in absorbance at 338 nm with the number of layers.

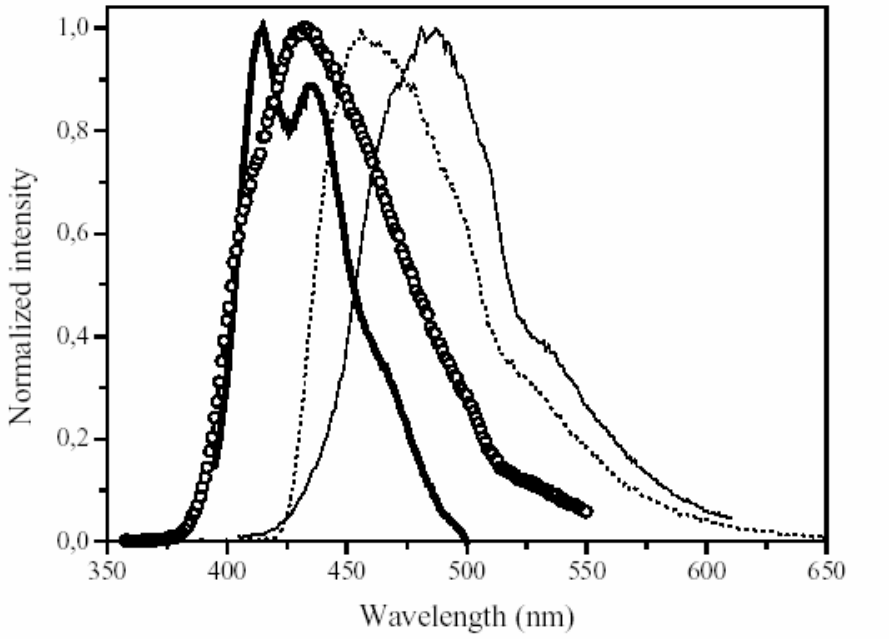

Figure 7. Fluorescence spectra of CBS in: aqueous solutions (10^{-7} mol L^{-1}) (-o-o-o) and (10^{-2} mol L^{-1}) (⋯), in a crystal (—) and adsorbed on cellulose fibers (—). λ_{exc} = 348 nm.

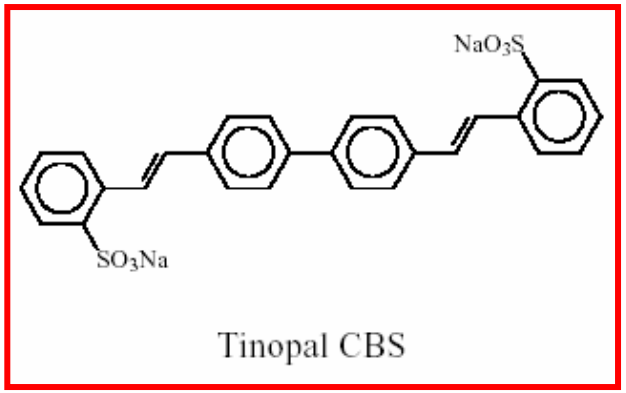

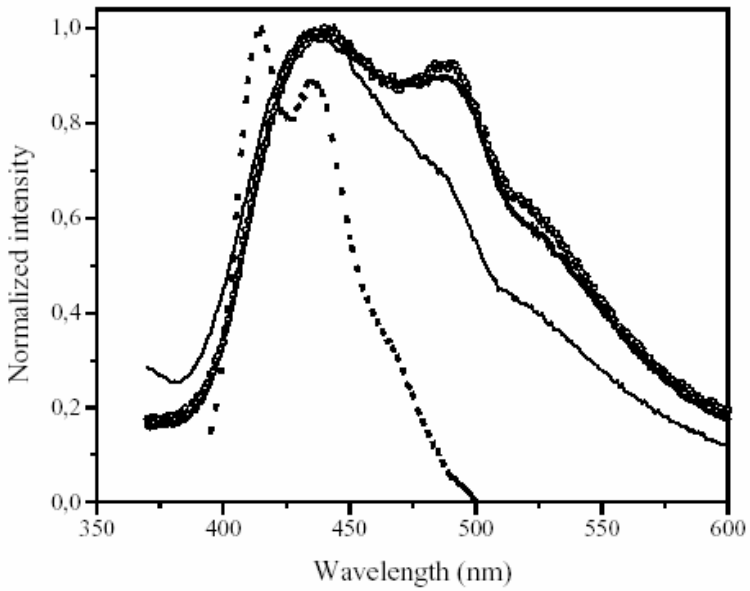

Figure 8. Fluorescence spectra of CBS adsorbed on cellulose fibers (----) and on LbL films prepared using dipping solution with pH 4.0 (-o-o-) and pH 10.0 right after deposition (——) and after 20 minutes (—).

Relaxation process and spectral broadening

Table 1. Some Properties of Native Polyethylene Films Employed

Symbol	Thickness (μm)[32]	T_m (K)[a]	T_g (K)[a]	Density (g/cm^3)	% Crystallinity[b]
PE32	32	368	—	0.900[32]	32 (12)
PE42	38	389, 394[c]	243	0.918	42 (42)
PE42[d]	42	383	—	—	42 (41)
PE76	13	403	—	0.952	76 (42)

[a] Heat flow maxima from endotherms of DSC (heating) thermograms.
[b] By X-ray diffraction. Values in parentheses from DSC analyses.
[c] A polymer blend; both heat flow maxima in DSC thermograms are reported.
[d] A native PE42 film bombarded with 7.0 MeV alpha particles at a dose of 120 kGy.

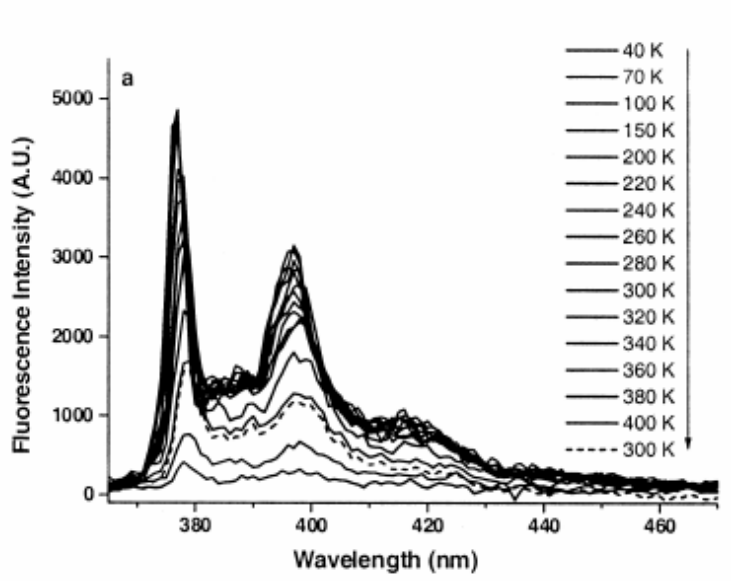

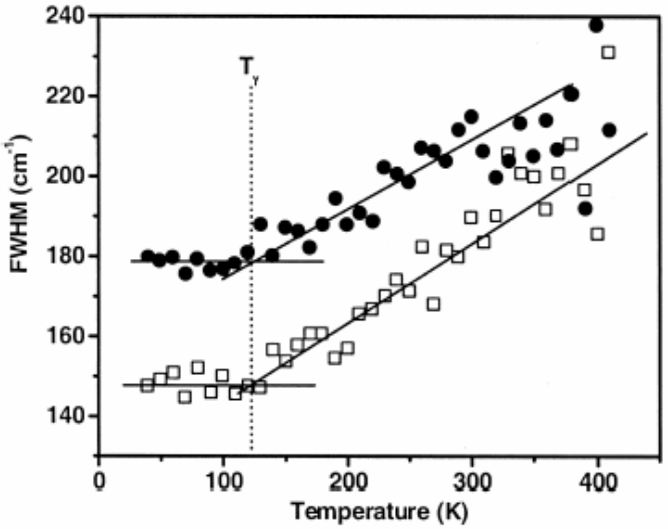

Figure 7 FWHM of the 1-pyrenyl 0–0 emission band from 10^{-2} mol/kg pyrene in **PE32** (●) and in **PE76** (□) films that were bombarded with 7.0 MeV alpha particles at doses = 110 (**PE32**) and 87 kGy (**PE76**). The vertical dotted line indicates the onset temperature for the γ-relaxation, based on the intersection of the best-fit straight line segments. The data for the **Py–PE32** sample have been offset by 30 cm^{-1} for clarity.

Brown, et.al. J. Polum Sci. Polym. Phys. Ed. 2004

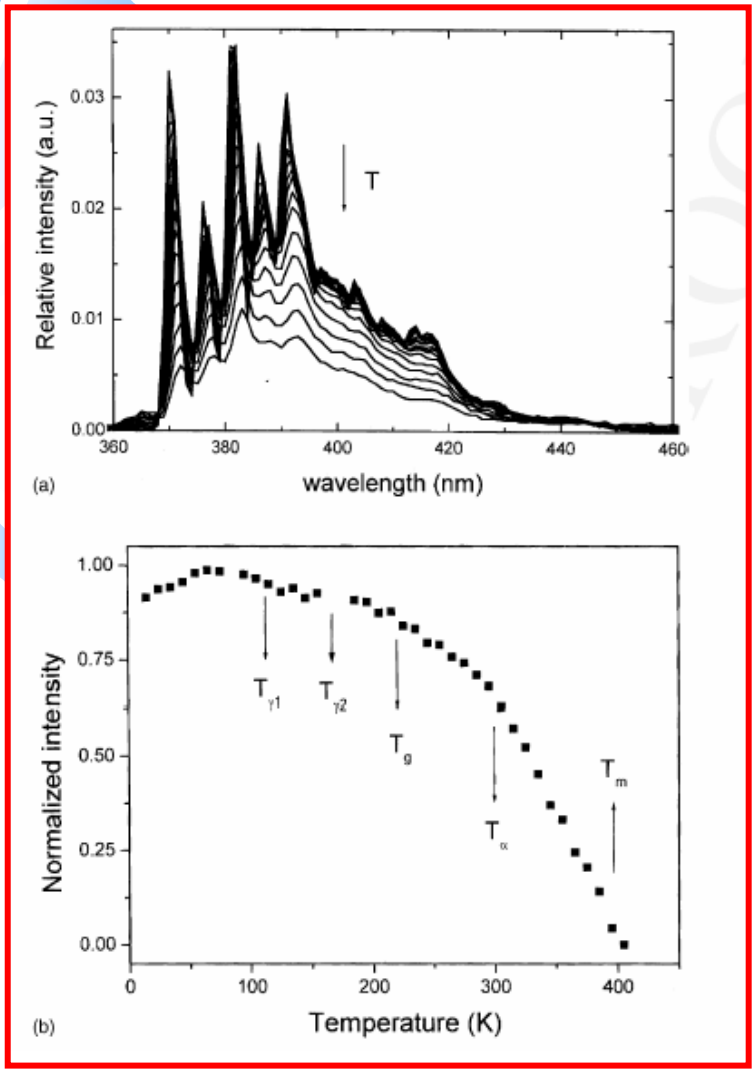

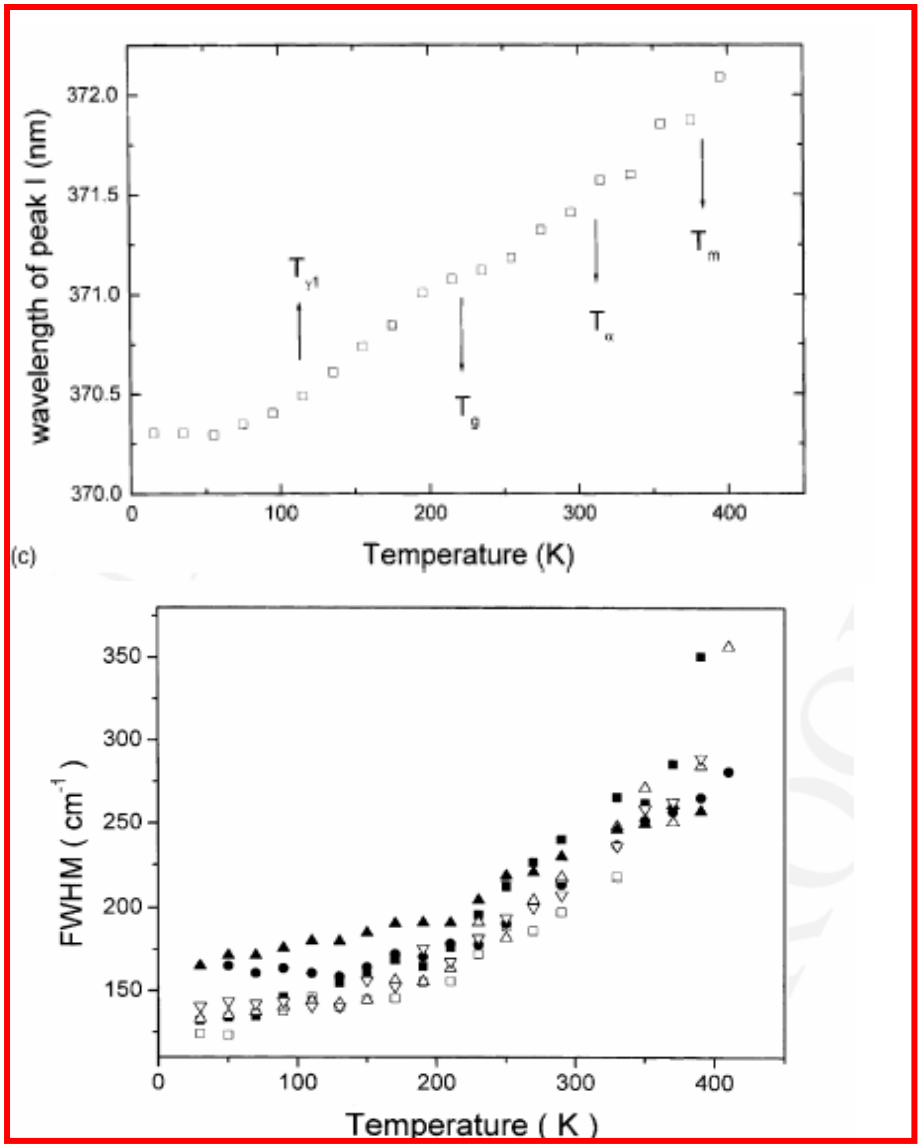

Fig. 1. (a) Fluorescence spectra of pyrene sorbed in HDPE; (b) integrated intensity of the fluorescence band; (c) wavelength of the vibrational band I (λ_{em} = 372–374 nm). Several temperatures between 15 and 405 K.

Martins, et. Al. J. Phochem. Photobiol. A Chem. 2002

Thank you!

Fred

Miguel

Jennifer